UiT
THE ARCTIC UNIVERSITY OF NORWAY

Faculty of Bioscience, Fisheries and Economics

Department of Arctic and Marine Biology

Influence of photoperiod on central appetite regulation in captive Svalbard rock ptarmigan (*Lagopus muta hyperborea)*

Vebjørn Jacobsen Melum

Bio-3950 Master thesis in biology, August 2018

Main supervisor: Gabriela Wagner (AMB, UiT)

Co-supervisor: Alexander West (AMB, UiT)

UNIVERSITETET I TROMSØ

Abstract

The Svalbard rock ptarmigan displays a seasonal change of body mass as a selectively beneficial adaptation for survival in the high Arctic. This physiological change is sensitive to photoperiod (daylight duration in a 24h cycle) but little is known of the mechanism through which changes in photoperiod affects body mass in this species. We exposed winer adapted Sv. rock ptarmigan to a simulated lengthening natural photoperiod (NP), constant light (LL), and constant darkness (DD). As expected, increasing photoperiod rapidly reduced body mass (BM), likely as a consequence of increased activity which occurred without compensation of increased voluntary food intake (VFI). Expression of the thyroid hormone metabolising enzyme Dio2 was quantified within the mediobasal hypothalamus (MBH), as an indicator of seasonal status. Similar to other seasonal models, Dio2 was stimulated by lengthening photoperiods and spontaneously induced by extended exposure to constant darkness. Expression of Dio2 was positively correlated with expression of NPY (a crucial appetite regulating peptide) within the Arcuate nucleus (ARC). Conversely, the expression profile of the closely associated orexigenic factor AgRP was correlated with BM, but not Dio2 levels. Expression of the satiety factor POMC was unaffected by photoperiodic changes. Collectively these data demonstrate that although photoperiod affects central gene expression in the Sv. Rock ptarmigan their expression does not directly dictate changes in VFI or BM. Instead, a more complicated pattern of appetite regulation emerges, processing photoperiodic and metabolic signals as well as seasonal behavioural changes in the Svalbard rock ptarmigan.

Keywords: Svalbard Rock ptarmigan, mediobasal hypothalamus, Dio2, AgRP, NPY, POMC

Table of contents

Preface

Two years of study are over. Through the work as a master student I have learned more than envisaged. To summarize it all would be another thesis. Of the most important I am now equipped with a diversity of tools and the ability to plan and execute an experiment to try to answer the questions of interest. This work would never have been achieved without the great people I am surrounded with. I would therefore like to use the opportunity to express my gratitude to the central of them.

I would like to thank Gabi for the opportunity to participate in this interesting project, sharing your genuine interest and knowledge of birds, guidance, and the trust to allow me work independently.

I would also like to thank Alex for our valuable discussions, thorough feedback, and your pedagogical skills in explaining molecular biology in a comprehensive way.

A special thanks to Daniel for all hours together being it with the birds, in the lab or in your office. The value of collaboration is now particularly clear to me.

Thanks to the institute technicians, Hans Lian, Renate Thorvaldsen and Hans Arne Solvang for guidance, discussions, help, and valuable input on the care of the animals.

Thanks to all members of the Arctic Chronobiology and Physiology research group for inspiring discussions and useful inputs throughout the study period.

Thanks to Eva Fuglei for the opportunity to study these magnificent birds in the wild.

Thanks to family and friends for their understanding and support.

Sanne, your patience and support is everything. You are the one that makes the everyday flow.

List of Abbreviations

AA: amino acid

Arc: arcuate nucleus

AgRP: agouti-related protein,

αMSH: alpha melanocyte stimulating hormone

BM: Body mass

CART: cocaine amphetamine responsive transcript

CCK: cholecystokinin

DD: constant darkness

DDc: constant darkness control group

DMH: dorsomedial hypothalamus

FFA: free fatty acids

FI: food intake

FIR: food incorporation rate

FLD: first long day

GABA: gamma-Aminobutyric acid

GLP1: glucagon-Like-Peptide 1

*IS*H: *in Situ* hybridization

LH: lateral hypothalamus

LL: constant light

LP: long photoperiod

MBH: mediobassal hypothalamus

MC3R: melanocortin 3 receptor

MC4R: melanocortin 4 receptor

NP: natural photoperiod

NPY: neuropeptide Y

POMC: proopiomelanocortin

PP: photoperiod

PT: pars tuberalis

PVN: paraventricular hypothalamus

RMR: resting Metabolic Rate

SEM: standard error of the mean

SP: short photoperiod

VFI: voluntary food intake

1 Introduction

1.1 The timing of biological life events

Predictable daily and yearly changes in the environment have created an evolutionary selection pressure that favours organisms which are able to exploit rhythmically changing environments. Resultantly almost all organisms have endogenous physiological timing mechanisms called biological clocks. The clock allows each organism to anticipate, and so achieve close synchronisation with, the rhythmic changes in the environment. Hence, specific behavioural and physiological traits can be expressed within an optimal temporal niche (Woelfle et al., 2004, Dodd et al., 2005). The mechanisms underpinning biological clocks and how they synchronise with the environment are still only partially understood. An overview of our current understanding is developed below.

1.1.1 Circadian rhythms

The Earth rotates on its axis every 24 hours rhythmically exposing the surface to the Sun (**Figure 1**). This dramatically changes the surface environment depending upon the time of day, particularly in terms of temperature, humidity, and light. Because of these daily changes it is important for organisms to have an inner sense of time that allow them to anticipate upcoming changes. An endogenously driven rhythmicity with a period of around 24 hours persists under constant conditions and is called a circadian rhythm.

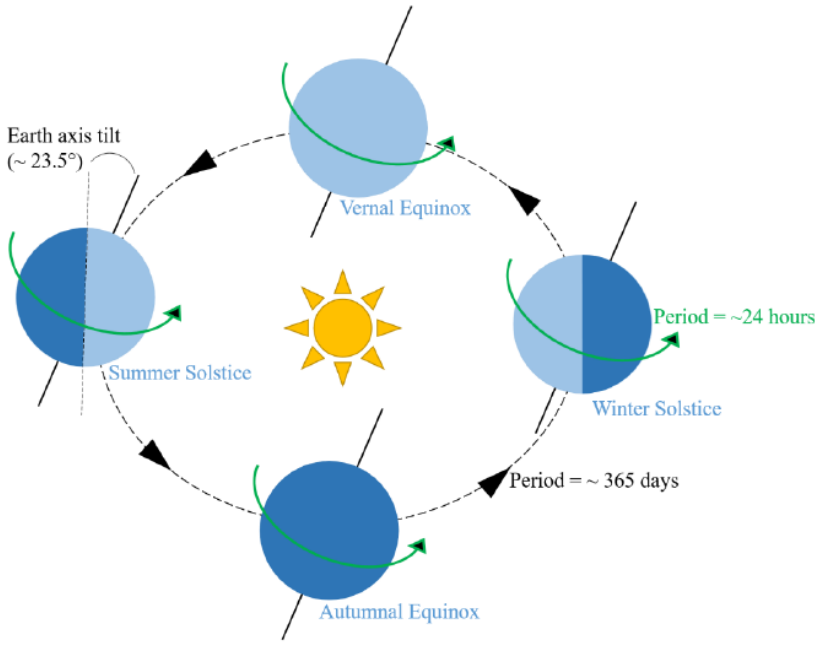

Figure 1 The earth`s orbit around the sun. The earths daily rotation around its own axis is creating the difference of day and night. Its yearly rotation around the sun is creating our four seasons. Further from the equator, the seasons become more pronounced. The earths tilt of 23.5° are during the winter months creating a polar night on the north pole lasting for 6 months before 6 months of continuous light are taking over. The same happens on the south pole just on the opposite time of year. Figure adapted after (Appenroth, 2016).

1.1.2 Seasonal rhythms

The Earth's yearly orbit around the Sun creates the four seasons (**Figure 1**). As latitude on the Earth's surface increases so too does the amplitude in changing daylight (photoperiod, PP) over the course of the year. This reaches the extremes at the poles where the 23.5 ° tilt of the earth causes the north and south poles to be 6 months in constant light in the summer and 6 months in constant darkness in the winter. As an adaptation to these seasonal changes in their environment animals have developed seasonal changes in physiology to optimize their evolutionary fitness. These rhythms are less studied because of their need for long term studies. Nevertheless, these rhythms are crucial for animals' survival, especially in arctic regions.

1.1.3 Light

Changes in weather fluctuate from year to year. Irradiance and temperature are therefore unstable proxies for the time of year. PP, on the other hand, is consistent year after year and therefore the most important Zeitgeber (entrainment factor; German for "time giver") for biological clocks.

Although PP is stable at a fixed geographical point from year to year, the change over the year depends on latitude. Figure 2 shows how these yearly changes in PP are differing with latitude. Focusing on the blue line representing 75°, equivalent to parts of Svalbard, PP is rapidly going from 0 hours in midwinter to 24 hours during the summer.

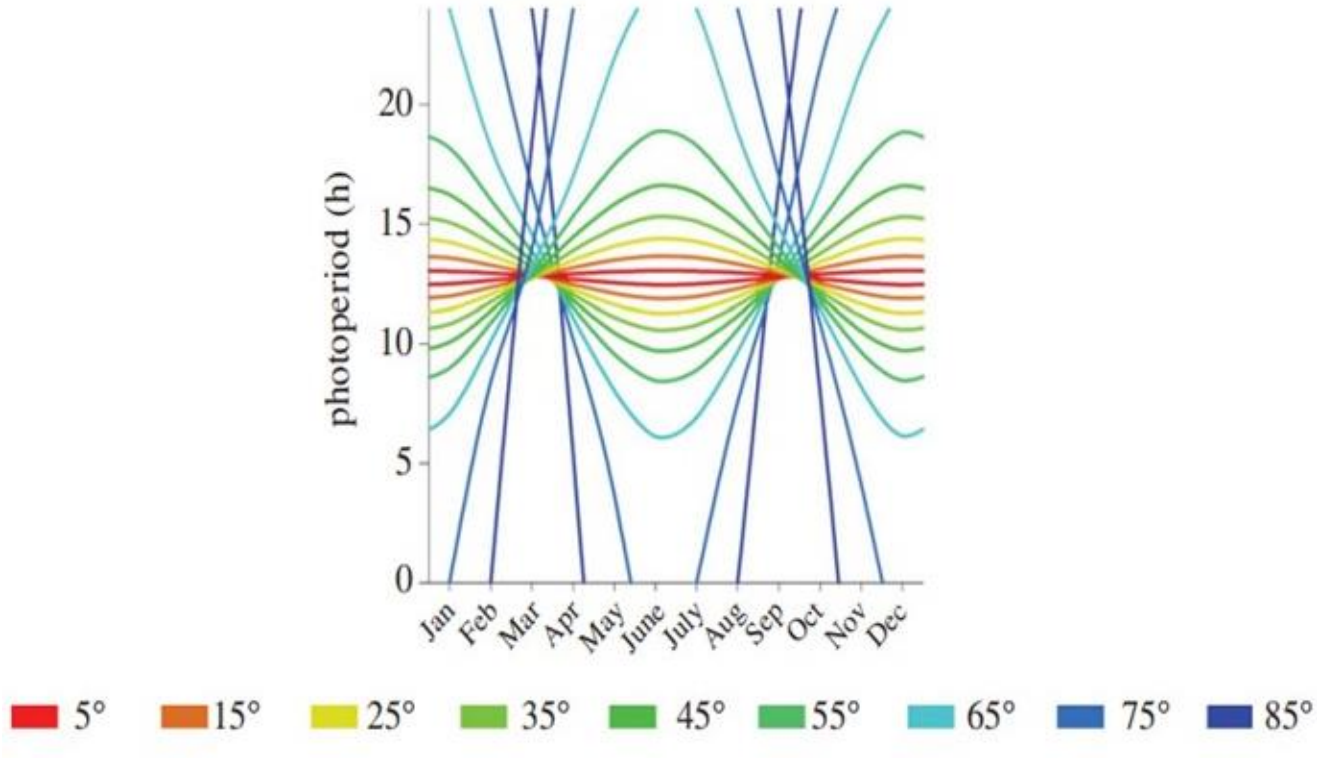

Figure 2 Latitudinal changes of twilight and PP. The figure shows the changes in PP. Coloured lines are representing different latitudes. Focusing on the colour representing 75° it is possible to appreciate the huge seasonal fluctuations in PP, from 24 hours in summer to 0 hours in midwinter. The figure is adapted after (Hut, Paolucci, Dor, Kyriacou, & Daan, 2013).

1.1.4 The circadian clock

The circadian rhythm are governed by a circadian clock, which is best studied in mammals. Within each mammalian cell there is a ~24h cycle of synthesis and degradation of clock-proteins which provides a framework for all temporally controlled cellular processes (Partch et al., 2014). This ~24h cycle is self-regulated through a transcription translation feedback loop (TTFL) and involves several genes. Genetic studies have shown one of the most important ones to be Circadian locomotor output cycles kaput (CLOCK), brain and muscle (aryl hydrocarbon receptor nuclear translocator-like protein 1 (ARNTL1)) (BMAL1), period (PER) and cryptochrome (CRY) (Partch et al., 2014). These four integral clock proteins work as two dimers. The CLOCK-BMAL1 dimer acts as an activator while the PER-CRY dimer act as a repressor. The cyclic transcription and translation of these genes with the help of kinases and phosphatases makes the robust 24-hour rhythm of gene expression (see **Figure 3**). The precise mechanisms by which the rhythmical gene expression couples to physiological and behavioural processes are still not yet fully understood.

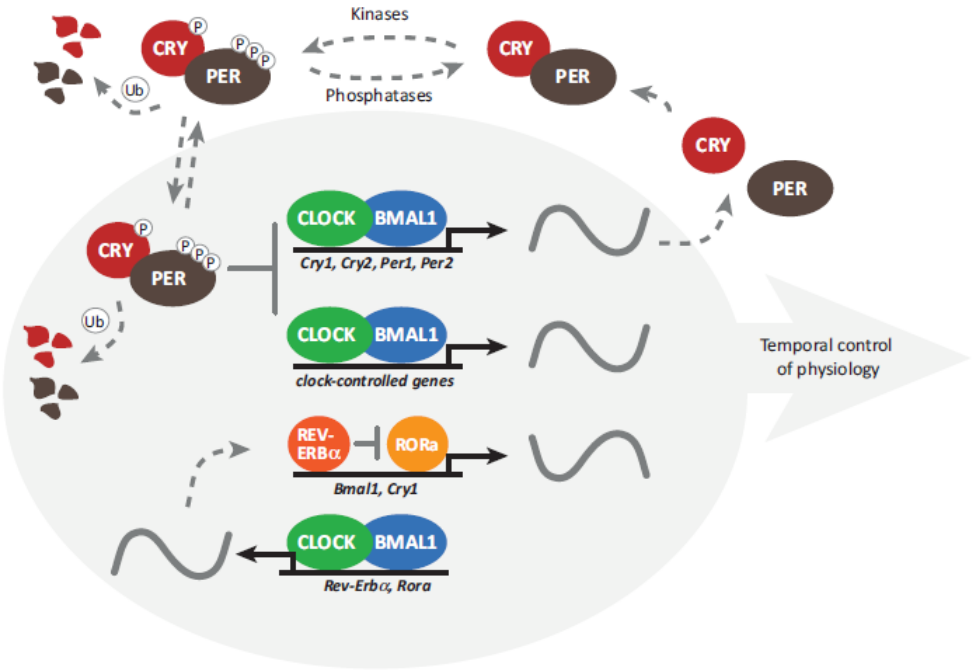

Figure 3 Transcription Translation Feedback Loop. Within each cell the four main integral clock proteins are involved in the cyclic 24-hour rhythm of gene expression. This is regulated through a negative feedback control where the concentrations of their product are reducing the production of the substrate required to make the end product, in this way limiting its own concentration. It is this cycle that takes roughly 24 hours and makes the endogenously sense of time. Figure adapted after (Partch et al., 2014).

In mammals peripheral clocks are synchronized by the master clock, the suprachiasmatic nucleus (SCN) of the hypothalamus, located in the brain, just above the crossings of the optic tracts. Multiple entrainment signals are controlled by the SCN, including glucocorticoids (Balsalobre et al., 2000), serum response factor, body temperature fluctuations, activity rhythms and the hormone melatonin, which is secreted from the pineal gland as a response to darkness. Different part of the body, depending on function, are differently sensitive to different factors (Panda et al., 2002). The melatonin duration is shown to be of different importance for the daily circadian synchronization in birds and mammals (Brandstätter, 2003, Bartness et al., 1993). Mammals do not require melatonin for circadian entrainment, as exemplified by the standard C57Bl6/J mouse which do not express the necessary enzymes to make melatonin, yet still synchronize their periphery effectively (von Gall et al., 1998). Conversely pineal

transplantation experiments in the house sparrow demonstrates that recipient birds immediately align to the donor birds circadian phase, thereby implicating melatonin is a strong circadian entrainment factor in birds (Binkley and Mosher, 1985, Heigl and Gwinner, 1995).

1.1.5 Avian seasonal timing

In avian species PP is sufficient to drive changes in seasonal phenotype. Long days induce a summer phenotype and an activation of the reproductive system. They are therefore characterized as long-day breeders. The PP effectively inducing a change in seasonal phenotype is termed the critical PP and it varies with latitude and species.

Thre is evidence to suggest that the photoperiodic timekeeping in birds requires a circadian framework. This is exemplified through the Nanda Hamner paradigms where photosensitive birds kept under short photoperiods were exposed to 8h pulses of light which arrived after differing extended periods of darkness. In these studies photoinduction is only achieved when environmental light is exposed to a photosensitive phase of an endogenous circadian oscillator (Follett et al., 1974, Nanda and Hamner, 1958).

The connection between circadian timekeeping and seasonal rhythms is theorised by two main hypotheses known as the external and internal coincidence models (Pittendrigh, 1972, Bünning, 1937). The internal coincidence model postulates that there is an internal rhythm of photosensitivity, divided into sensitive (photophile) and insensitive (scotophile) phases. Light applied during an insensitive phase remains without effect on the internal timing, while light applied during a photosensitive phase will trigger a long day phenotype. It is therefore not the duration of light experienced by an animal which is important for inducing a long day response, but at which phase the organism experiences light in relation to its internal ~24h rhythm of photosensitivity (Bünning, 1937, Follett et al., 1974). External coincidence model supposes that there are two cohorts of factors, one coupled to dawn and the second to dusk. As PP changes the phase relationship (number of hours between dawn and dusk) between the cohorts change and this association is interpreted by the organism. This is supported by experiments in mammals (Wagner et al., 2008). Although both models are useful conceptual tools at present there is insufficient evidence to support the mechanistic existence of either the internal, external, or alternative models.

The light signal in mammals is only perceived through the eyes. With the use of the light sensing ganglion cells in the retina the SCN is informed whether it is light or dark outside. The SCN further communicates with the pineal gland which secretes melatonin during darkness. Hence the duration of melatonin within a 24h cycle accurately reflects the time of year (**Figure 4**). Seasonal changes in melatonin duration lead directly to locally seasonal changes in thyroid stimulating hormone (TSH) in the pars tuberalis (PT) (Bartness et al., 1993). This seasonal change of TSH in the PT inducing ependymal cells (ECs) (also called tanycytes) lining the third ventricle to up or downregulate the metabolism of the bioactive hormone Triiodothyronine (T3) from the inactive prohormone thyroxine (T4) by changing the transcription activity of an enzyme called type 2 deiodinase (DIO2) (Yoshimura et al., 2003). The seasonal change in T3 is responsible for morphological changes in the gonadotropin releasing hormone (GnRH) nerve terminals that increase GnRH secretion, leading to gonadal development (Nakao et al., 2008). Recent work on seasonal changes of Dio2 in the PT supports the applicability of the findings in the japanese quail to the Sv. rock ptarmigan (Appenroth, 2017). The response that occurs in the PT depends on the species´ seasonal reproduction strategy. In contrast to mammals, the avian brain is penetrated by light and both the pineal gland and deep brain photoreceptors (DBP) can sense changes in light intensity and duration (Nakane et al., 2010). The DBP signal directly

to the PT and inhibit or induce TSH production depending on time of year. Impressively the downstream pathway from the PT is similar in both birds and mammals highlighting the deeply conserved nature of photoperiodic timekeeping in vertebrates (Nakane and Yoshimura, 2014).

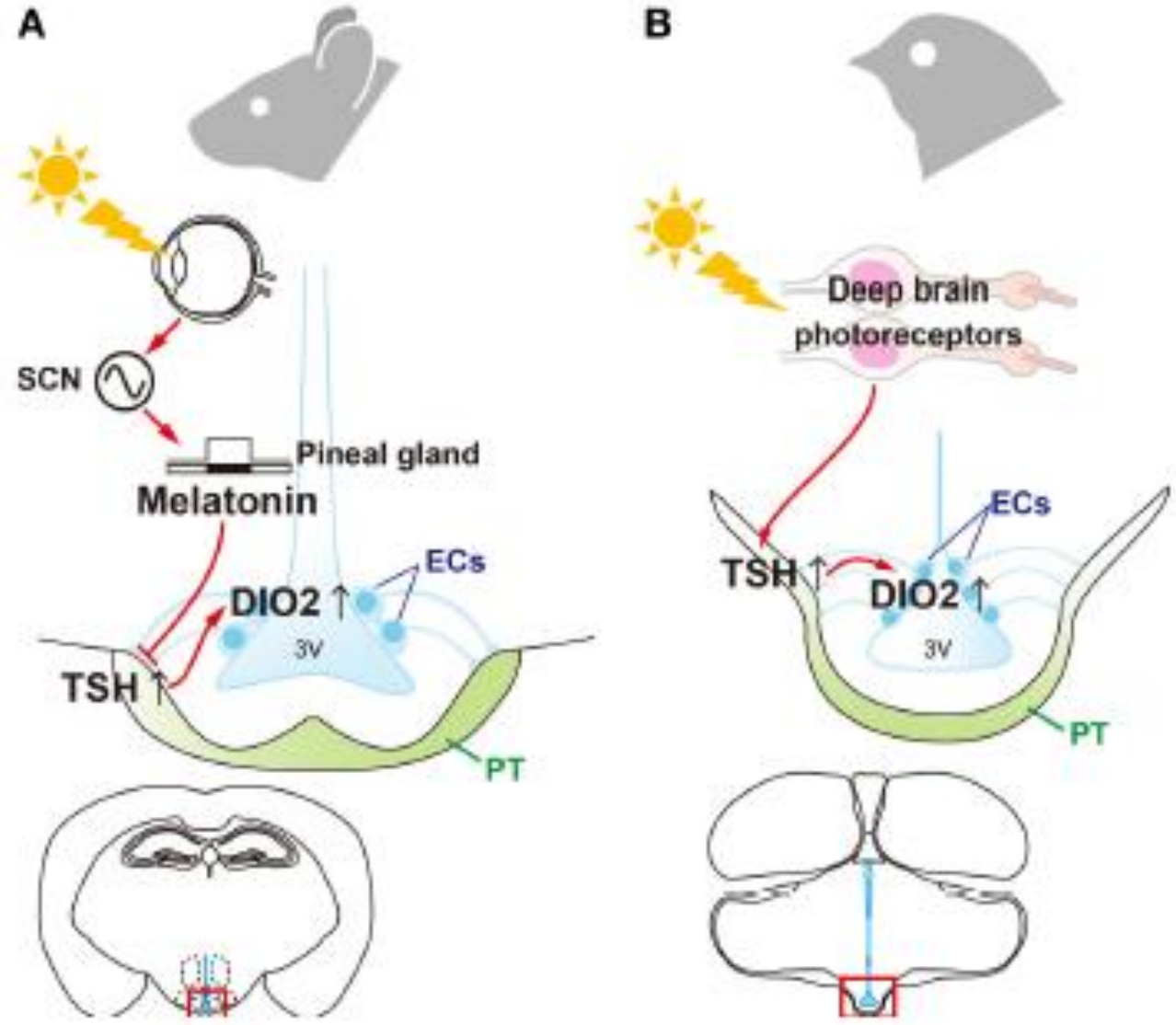

Figure 4 Photoperiodic signal pathways. The figure show similarities and differences in how photoperiodic signals are transmitted and translated in A: mammals and B: birds. The light signal is in mammals only perceived through the eyes. The photoperiodic signal travels to SCN which further communicates with ependymal cells in the pars tuberalis (PT) through the duration of melatonin produced from the pineal gland. This changes gene expression levels of TSHb and DIO2 and leads to a seasonal physiological response. In avian species deep brain photoreceptors are also susceptible to light. They transmit the signal directly to the ependymal cells. The further down-stream processes are similar as in mammals. Figure adapted after (Nakane and Yoshimura, 2014).

1.2 Svalbard

1.2.1 An archipelago in the high Arctic

Geographically the Arctic is the area of the globe north of the Arctic circle, where 1 day of continuous light occurs in the summer. The Arctic can be defined in many other ways, including the distribution of vegetation, precipitation or temperature. Temperature is frequently used as a defining factor as it limits plant growth, thus affecting the entire ecosystem. Throughout this thesis, the Arctic is defined as the region above the 10°C isotherm, along which the maximum average temperature in the warmest period of the year (July) does not exceed 10 °C.

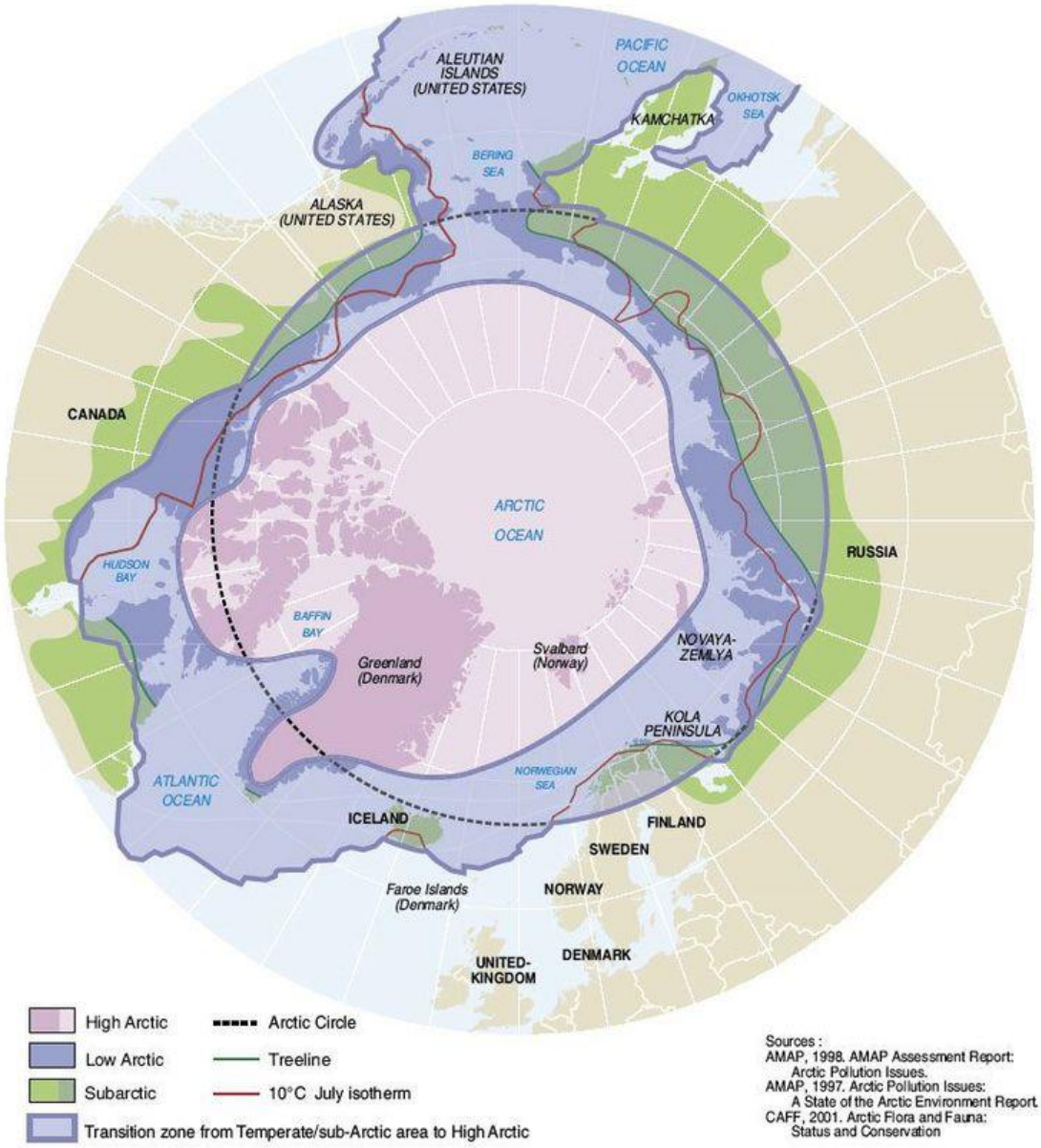

Figure 5 Definitions of the Arctic. The most common criteria are the Arctic circle (1 day of continuous light during summer), the treeline (where the treeline ends), and the 10°C July isotherm (where the maximum temperature in July does not exceeds 10°C). Figure adapted after AMAP 1998.

1.2.2 Characteristics of Svalbard

The Arctic is, because of the positioning towards the pole, an environment with large seasonal changes both in temperature, light intensity, and biomass. These extreme seasonal changes in light makes the resident animals especially interesting to study adaptations to circadian and seasonal chronobiology. To better appreciate the environment the resident animals live in on Svalbard, a characterization of the regions temperature and climate is described below.

Svalbard is an archipelago in the high arctic creating one of the northernmost terrestrial ecosystems of the world. It is consisting of numerous islands, ranging from 74-81°N, 15-30° E and covering 62 700 km^2, with Spitsbergen (37 700 km^2) is being the largest (Ims, 2014).

The arctic climate is often cold and dry and Svalbard is no exception to this. Other than regions at a comparable latittude, the movement of warm air and the north Atlantic Sea give the west coast of the archipelago milder temperatures and make it usually ice-free during the winter. These milder periods characterize the winter, and events of rain on snow are of crucial importance for the resident animals (Ims, 2014). Despite this, the average temperature for the west coast of Spitsbergen (Longyearbyen airport) was -6.7°C from 1961-1990. The average precipitation is varying annually from 500 mm in the outer parts of the fjords on the west coast to 200 mm in the inner parts of these fjords (E. J. Førland (ed) et al., 2009).

Because of the harsh environment, Svalbard has only four resident animals: two herbivorous mammals, the indigenous Svalbard reindeer (*Rangifer tarandus platyrhynchus*) and the introduced local population of the Sibling vole (*Microtus levis*) around Longyearbyen, one herbivorous bird, the Svalbard rock ptarmigan, and the Arctic fox (*Vulpes lagopus) as* the only resident predator.

Figure 6 Rocky country. The picture is taken towards the Adventvalley from the Baltervalley and illustrates the rough and barren country even at its most plentiful time of year.

Svalbard is populated by a small number of specialist arctic plant species. Trees are a minor feature of the habitat with only the dwarf birch (*Betula nana*), which presents as a low growing shrub, indigenous to this region. Mountains, rivers, valleys and rocks dominate the landscape. The food plants that are important for the Svalbard ptarmigan are found in between the rocks and consist mainly of polar willow (*Salix polaris*), mountain sorrel (*Oxyria digyna*), alpine bistort (*Bistorta vivipara*), different species of the family blue- (*Poa sp.)* and tussock grass (*Deschampsia sp.)*, purple saxifrage (*Saxifraga oppositifolia)* and tufted saxifrage *(Saxifraga cespitosa)*. Arctic bell-heather (*Cassiope tetragona*) is not considered to be an important food plant, but it has been observed to be eaten by adult males in August (personal observation).

Figure 7 Alpine bistort (Bistorta vivipara). Important food plant for the Svalbard ptarmigan during the fattening in the summer and early fall because of its high protein content.

During the winter months, the access to food varies highly with snow cover, and the resident animals have evolved comparable strategies to survive the winter, including seasonal cycles in moult, fat deposition and metabolic rate. The physiological changes undergone by the Svalbard rock ptarmigan are described in more detail below.

1.3 Seasonal changes in the physiology of the Svalbard rock ptarmigan

The Sv. rock ptarmigan goes through seasonal changes in physiology and behaviour to meet the requirements of the environment for survival. One unique adaptation, only seen in the subspecies Svalbard rock ptarmigan, is the capacity to deposit up to 35 percent of BM as fat (Mortensen et al., 1983).This ability is likely to have evolved as a solution to periods with climatic conditions limiting food availability (Stokkan, 1992). The previously documented seasonal changes in physiology and behaviour of the Sv. rock ptarmigan is further investigated in the context of energy balance and central regulation of appetite and food intake.

1.3.1 Appetite regulation

One requirement for the survival of the Svalbard rock ptarmigan is to meet its energetical demand. Available and expended energy determine the energetical state of the bird. In general, energy balance can be broken down into three major components: 1) appetite and food intake, 2) energy storage and 3) energy expenditure (Morton et al., 2006). If the ptarmigan has higher energy requirements than energy consumed it is in a negative energy balance and it will start to catabolize its own cells to meet the energetical demand. A positive energy balance occurs if the ptarmigan ingests more energy than it requires. A positive energy balance is characterized by an anabolic state with the deposition of energy storage. Animals in Arctic environments have evolved the ability to deposit fat as an energy store in anticipation of seasonal food shortage and low temperatures (Blix, 2016). To time this upregulation of body mass the animals need a mechanism to relate appropriate body mass to the time of year and upcoming environmental changes.

1.3.2 Sliding set point theory

In 1970 Mrosovsky *et al.* postulated that ground squirrels regulate their body weight at a progressively declining level through their hibernation period. With this idea the theory of a sliding set point rather than a fixed set point could explain how animals with seasonal changes in body weight was able to fine-tune their seasonal appropriate body weight (Mrosovsky and Fisher, 1970).

Experiments performed by Mortensen *et al.* show how starved Sv. rock ptarmigan, when allowed to re-feed, eat more than the control group, but stop to eat more when their body weight reaches the seasonally appropriate weight as the control group (**Figure 8**) (Mortensen and Blix, 1985). This implies that bodyweight is controlled with reference to the time of year. PP is known to be a key cue to synchronize physiology with the environment (Brandstätter, 2003). Similar experiments in Djungarian hamster (*Phodopus sungorus*) have drawn the same conclusions (Steinlechner et al., 1983).

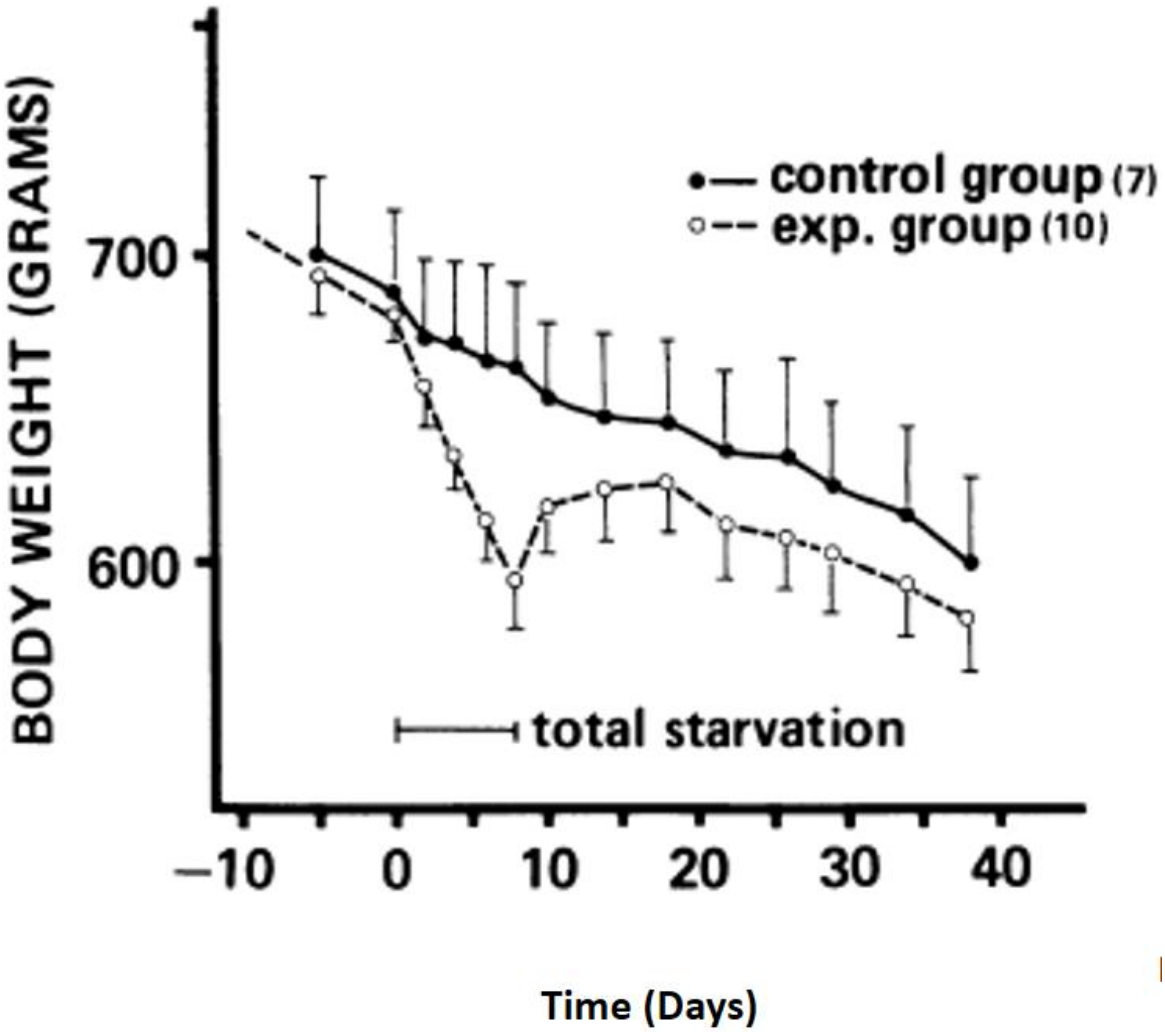

Figure 8 Starved Svalbard rock ptarmigan display a sliding set point of body weight. Svalbard rock ptarmigan lost weight after starvation for 7 days (open circles) during winter. Despite ad libitum access to food thereafter, body weight did not overshoot that of the control group (closed circles). Figure adapted after (Mortensen and Blix, 1985).

1.3.3 Impact of photoperiod on physiology of the Svalbard rock ptarmigan

To explain a change in body mass energy balance must be either positive or negative. Lindgård et al. report that under stimulated natural PP (NP) body mass (BM) rapidly increases in August and September until it reaches a plateau in October (**Figure 9A** (Lindgård et al., 1995). In the same period voluntary food intake (VFI) doubles (**Figure 9B**), while activity level decreases (**Figure 9C**). This suggests that the increased VFI and the decreased activity are the main drivers for the rapid BM increase in the fall. Further the BM remains constant from October to January (**Figure 9A**). Correspondingly the VFI drops (**Figure 9B**) and activity remain unchanged (**Figure 9C**). Since up to 32 % of the increase in BM can be fat (Mortensen et al., 1983) and the resting metabolic rate is reduced by more than 20 percent in winter (Mortensen and Blix, 1986) the continuation of the elevated BM can be explained even with a decrease in VFI. From January onwards BM decreases (**Figure 9A**) as activity levels increases (**Figure 9C**). It is worth noting the activity peak in April which leads to a more rapid decrease in BM. This increase in activity corresponds to the behaviour observed in the wild when both males and females spend an increased amount of energy and time on courtship, establishing a territory and chasing off competitors. From mid-late April pairs are established and devote more time to feeding, an observation which is conserved under lab conditions (Figure 8B&C, (Unander and Steen, 1985). This increase in VFI in May makes the BM to stabilize for a short period before a further decrease (**Figure 9B**). In the same period the females start to moult (Stokkan et al., 1986), which is an energetically costly process.

The measurements shown in **Figure 9** were obtained using captive ptarmigan held in Tromsø with one group under a simulated natural PP and one under constant light (LL). Both groups show a pronounced increase in body mass, the physiological preparation for winter. This indicates an underlying long-term timing mechanism in the LL group which makes these birds unresponsive to the ongoing photoperiodic summer signal. Such photorefractoriness can also be observed in great tits (*Parus major)* which stop breeding under an extended long photoperiod. Great tits from different latitudes were exposed to LD 13:11 for 123 days at two different temperatures. The influence of temperature on the onset of photorefractoriness differed with the latitude of tit origin (Stokkan et al., 1982, Silverin et al., 2008).

Despite the common underlying mechanism that governs the development of photorefractoriness, there are several differences between the LL and the NP groups. First, the LL group increases its BM at a slower pace than the NP group from September to October (**Figure 9A**). This can be explained by a decrease in VFI in the same period (**Figure 9B**) and a higher activity level (**Figure 9C**). Further, the stable elevated BM in October to December persist as in the NP group, but at a lower level (**Figure 9A**). From here on, the LL group increases its BM from December to February, where the NP group decrease (**Figure 9A**). Simultaneous the VFI drops from ~40 to ~30 grams (**Figure 9B**) and activity decreases from December to January before increasing again from January to February (**Figure 9C**). The increase in BM from December to January aligns with the changes in VFI and activity. The further increase from January to February is more difficult to explain with just the VFI and activity data provided by this study. One possible explanation could be that the PP delayed the birds change in resting metabolic rate (RMR). When this finally developed in January, the drop by 20 percent RMR can account for the BM increase even when VFI and activity alone should predict a stable or decreasing weight. From March to May BM remained elevated (**Figure 9A**), VFI almost doubles (**Figure 9B**) and activity levels are constant (**Figure 9C**). These parameters suggest an elevated BM if the allocation of the VFI or the RMR have changed during the experiment. Since the birds are under constant conditions these changes must be endogenously driven.

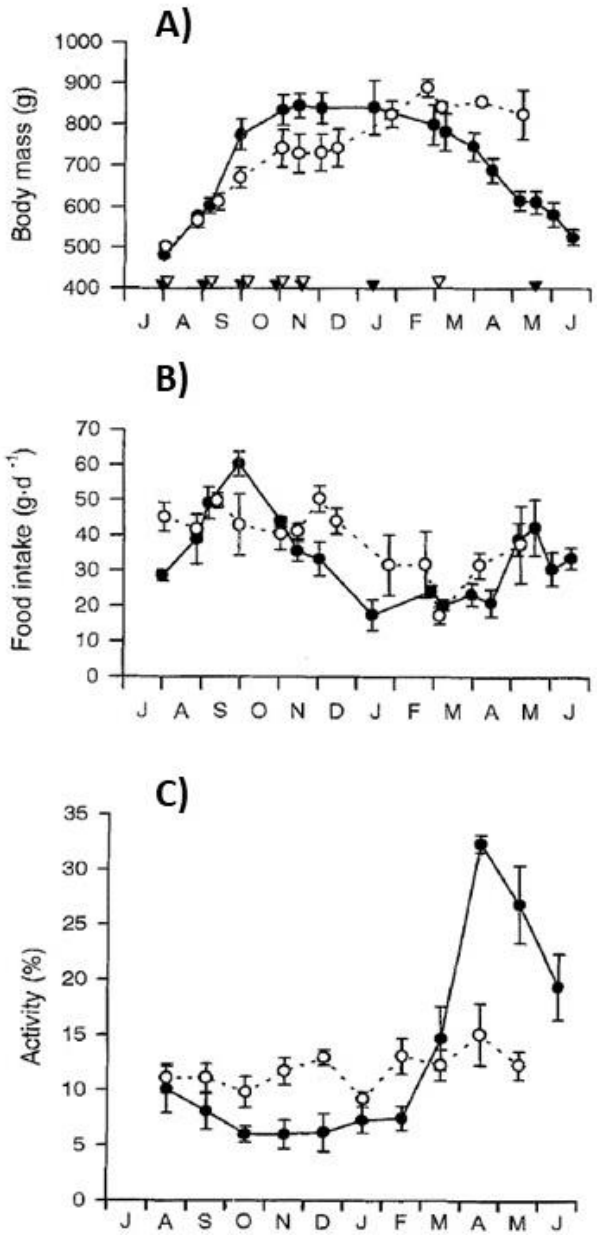

Figure 9 Yearly changes of body mass, food intake and activity. The three figures show the yearly changes of (A) body mass (grams), (B) voluntary food intake (grams/day) and (C) activity (mean monthly locomotor activity) in four captive birds exposed to simulated natural PP (closed circles) and continuous light (open circles) respectively, starting in July. Figure adapted after (Lindgård et al., 1995).

1.3.4 Control of food intake

For the brain to be able to regulate the periphery it needs to receive information on the peripheral status. This two-way communication between the brain and the periphery highlights the importance of understanding the signal pathways in both directions.

1.3.4.1 Peripheral input to the brain

The brain receives information, influencing the central regulation of appetite, from the peripheral system through several pathways. These pathways are best described in mammals and are divided into orexigenic (hunger) and anorexigenic (satiety, (Schwartz et al., 2000). The most important anorexigenic signals comes from leptin secreted from the adipocytes, insulin and Amylin; secreted by ß-cell in the pancreas and Cholecystokinin (CCK) a peptide hormone secreted in the gastrointestinal tract to induce fat and protein digestion. Opposingly, Ghrelin secreted from the ghrelinergic cells in the stomach, glucocorticoids such as Cortisol and Glucagon-Like-Peptide 1 (GLP1) are important peripheral signals stimulating an orexigenic response in the central appetite regulation in the brain (Marcelo and Horvath, 2012). In addition, metabolites such as free fatty acids (FFA), glucose and amino acids (AA) are registered and used as indicators for nutrient availability at different places in the periphery (Marcelo and Horvath, 2012, Schwartz et al., 2000).

In avian species the influence of peripheral signals on appetite regulation is less well documented. Glucocorticoids are shown to exert the same orexigenic responses seen in mammals (**Figure 10**) (Boswell and Dunn, 2017). In contrast, Ghrelin, known in mammals to stimulate hunger, are in neonatal chicks shown to induce an anorexigenic response when centrally injected (Furuse et al., 2001). Comparable to mammals, insulin and CCK induce an anorexigenic response when centrally injected in chicken (Honda et al., 2007, Denbow and Myers, 1982). The avian leptin was recently discovered and it`s function seems to differ from that in mammals (Seroussi et al., 2016). The hypothalamic level of T3 is a key determinant of annual weight regulation in the Siberian hamster (Murphy and Ebling, 2011). Because systemic levels of T3 and T4 are involved in many processes, the mechanisms these systemic fluctuations influence are difficult to test. It is therefore not feasible to compare the hypothalamic levels of T3 with systemic levels. However, the systemic plasma levels of T3 and T4 in the Sv. Rock ptarmigan show a seasonal fluctuation and differ with gender (Stokkan et al., 1985). Selected fat and lean chicken lines differed in their systemic plasma levels of T3 which may indicate its potential role in energy homeostasis (Byerly et al., 2009).

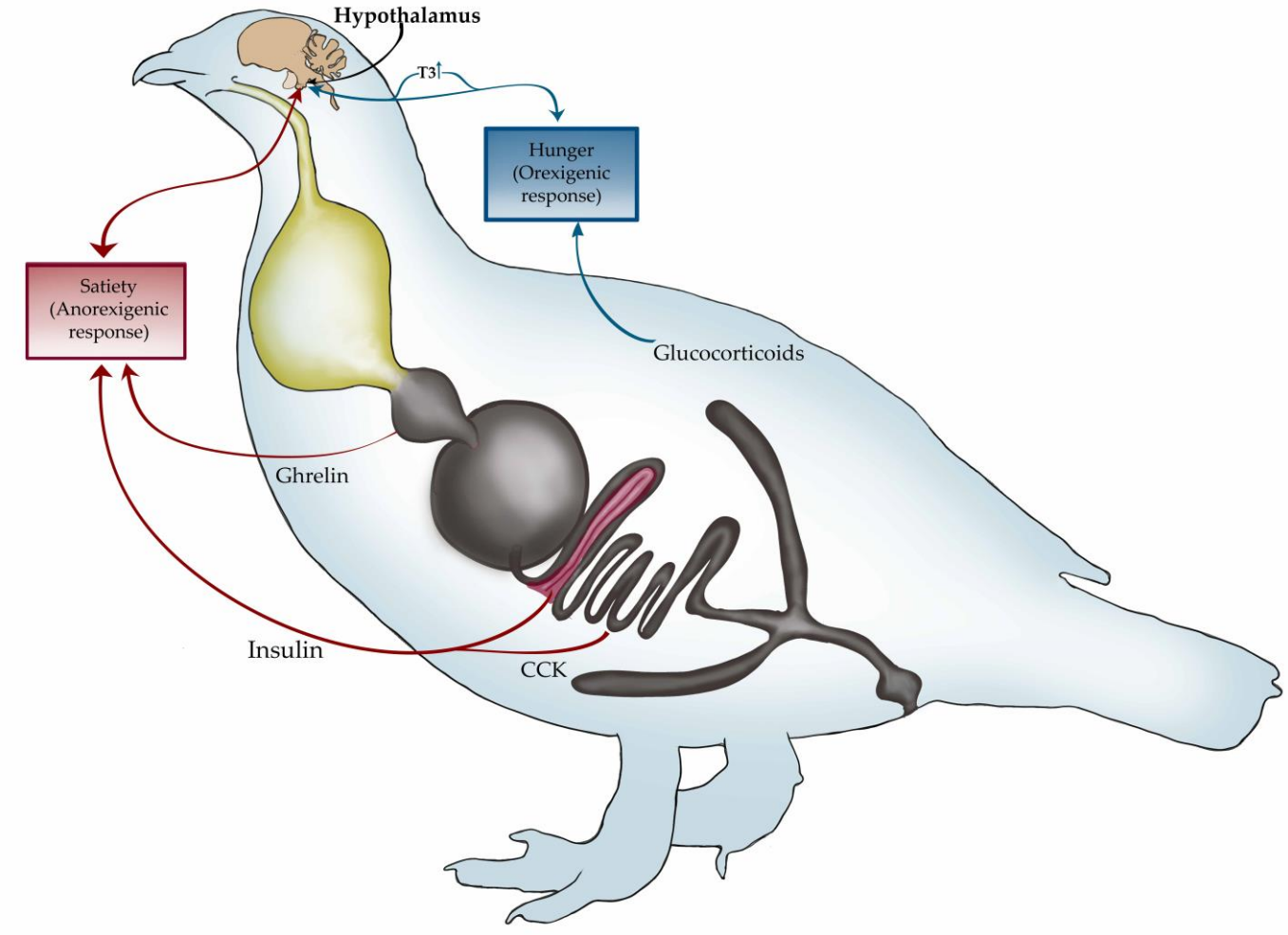

Figure 10 Peripheral signal pathways to the brain. Known peripheral signals involved in central appetite regulation in avian species. The pathways are divided into orexigenic responses (hunger) and anorexigenic responses (satiety). Glucocorticoids and increased hypothalamic levels of T3 induce an orexigenic response. Opposingly ghrelin, insulin and Cholecystokinin (CCK) exert an anorexigenic response in avian species. Figure made by Fredrik Markussen.

1.3.4.2 Control of energy homeostasis

The hypothalamus is central to energy homeostasis (Morton et al., 2006) by integrating peripheral input such as hormones, glucose and metabolites in the bloodstream for the brain's assessment of body condition. The input received in the brain influences the signal pathways controlling the periphery.

Within the mammalian and avian hypothalamus there are several regions important for energy homeostasis including the paraventricular hypothalamus (PVN), dorsomedial hypothalamus (DMH), lateral hypothalamus (LH), arcuate nucleus (ARC) and ependyma (**Figure 11,** (Andermann and Lowell, 2017, Boswell and Dunn, 2017). These areas are connected with neurons that stimulate and inhibit each other depending on the peripheral input. Of these areas the ARC is demonstrated to be the key centre for energy homeostasis with both function and anatomy well conserved in the mammalian and avian species that are investigated (Boswell and Dunn, 2017).

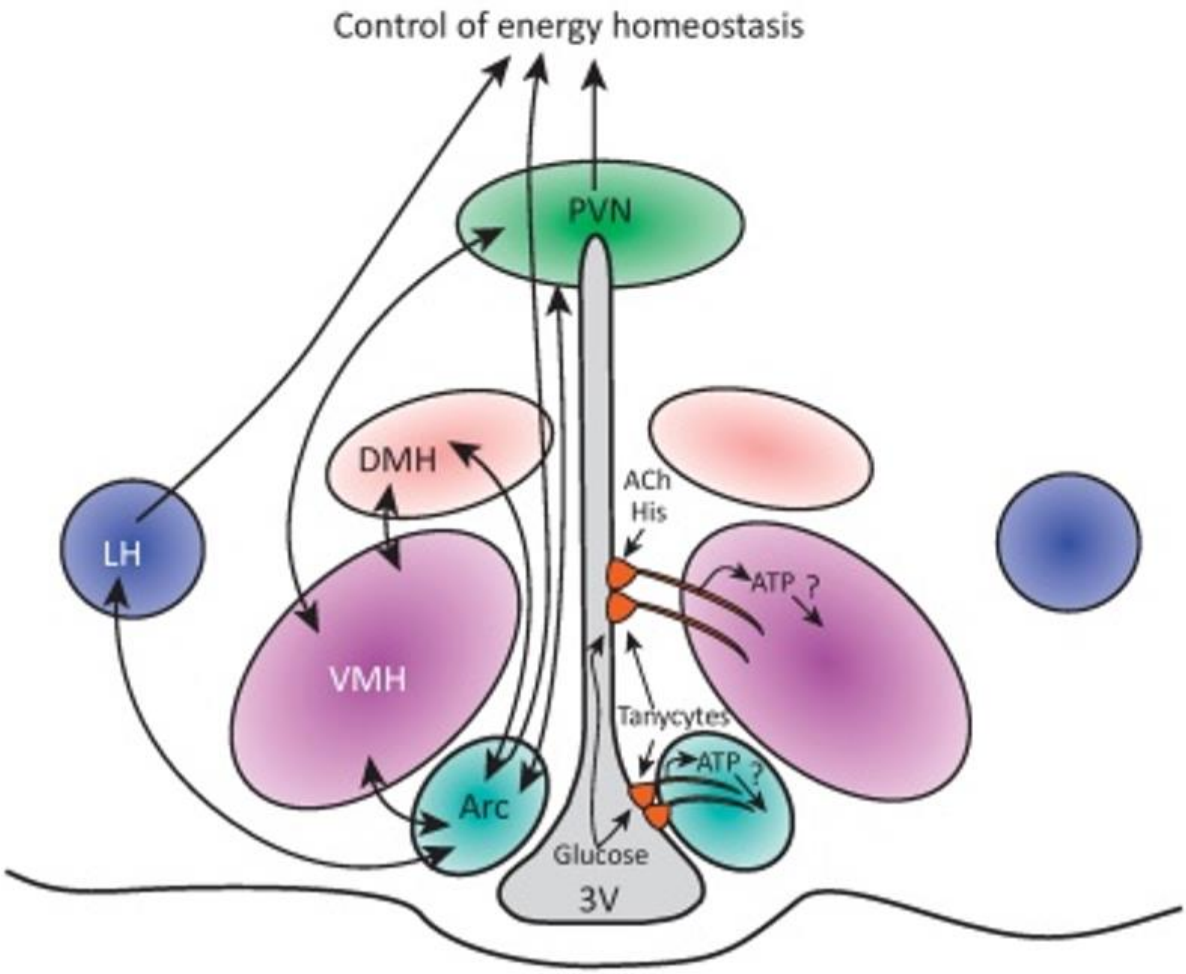

Figure 11 Brain regions regulating energy homeostasis. A cross-section of the hypothalamus showing brain regions involved in mammalian energy homeostasis. Adapted after (Bolborea and Dale, 2013).

The basis for neurological control is the integration of the brain`s signals from the body. The body weight status with regard to the time of year and the daily food intake in relation to the body weight status is all being sensed in the brain and the feedback from these signals is determining the output from the brain to the body to alter feeding behaviour, energy expenditure and activity levels.

1.3.4.3 First order control of energy homeostasis

The ARC consists of two types of "first order" neurons:

1) Orexigenic NPY/AgRP neurons stimulate hunger by releasing NPY, AgRP and GABA when ghrelin concentrations in the cerebrospinal fluid (CSF) increase, and leptin concentrations decrease. This leads to an inhibition on the MC4R neurons.
2) Anorexigenic POMC/CART neurons stimulate satiety by releasing αMSH (a peptide derivate from POMC) when ghrelin concentrations in CSF decrease, and leptin concentrations increase. This stimulates MC4R neurons.

The NPY/AgRP and POMC/CART neuron projects out of the ARC and influence different brain regions. Of highly importance is the projection to the "second order" neuron MC4R (**Figure 12**). The MC4R neurons receive input from POMC/CART and NPY AgRP neurons and regulate energy balance through downstream pathways.

Both the peripheral signal pathways and the central appetite regulators are highly conserved across vertebrate taxa (Boswell and Takeuchi, 2005, Yuan et al., 2017, Boswell and Dunn, 2017). Most of the avian work have been done on chicken (*Gallus gallus domesticus)* and Japanese quail (*Coturnix japonica*). Both species show increased gene expression of agouti-related peptide (AgRP) and neuropeptide Y (NPY) in response to fasting, but not pro-opiomelanocortin (POMC) (Song et al., 2012, Phillips-Singh et al., 2003). In addition, an increase of T3 levels in the chicken is shown to cause an increase in AgRP expression, an orexigenic response, and a decrease in POMC and leptin receptor, an anorexigenic response in the hypothalamus both *in vivo* and *in vitro* (Byerly et al., 2009). Through the interactions between these neurons the ARC integrates peripheral signals from the body and controls downstream physiology. This makes it an obvious place to start investigate seasonal changes in appetite regulation.

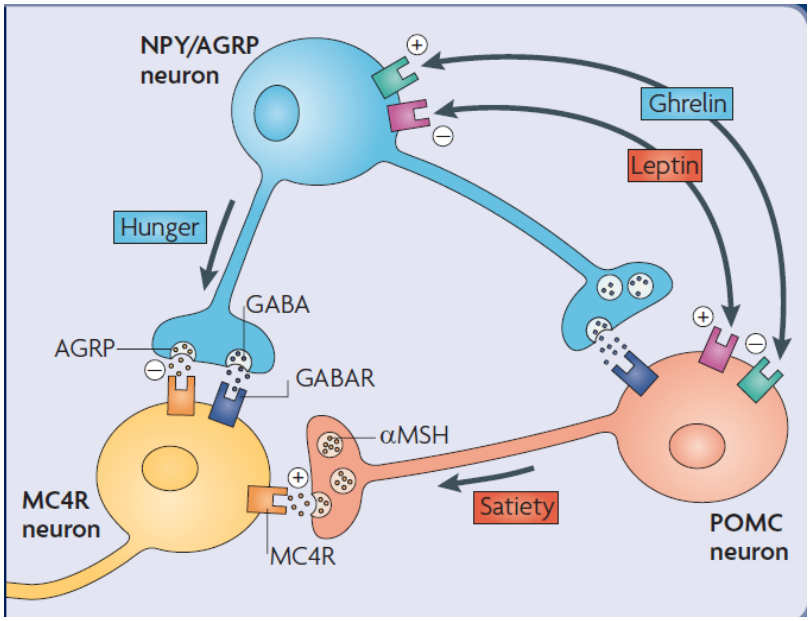

Figure 12 First order neurons in the arcuate nucleus project to the second order MC4R neuron. The simplistic schematic highlights the connection between the 1. order neuron NPY/AgRP and POMC/CART in the ARC and the 2. Order neuron MC4R outside the ARC. Abbreviations: NPY: neuropeptide Y, AgRP: Agouti Related Protein, GABA: gamma-Aminobutyric acid, POMC: proopiomelanocortin, αMSH: alpha melanocyte stimulating hormone, MC4R: melanocortin 4 receptor. Figure adapted after (Marcelo and Horvath, 2010)

1.4 Aim of the study

Several studies on Svalbard rock ptarmigan both in the wild and in captivity have provided a sound characterization of the relationship between photoperiod, physiology, and endocrinology. This makes the Sv. rock ptarmigan a useful model to investigate the effect of photoperiod on central gene expression in several ways:

1) Sv. rock ptarmigan display seasonal changes in body mass in captivity

2) Long term internal timing mechanisms are active in Sv. rock ptarmigan

3) They can be bred and kept in captivity in reasonably good numbers

4) They can be kept under controlled laboratory conditions which simplifies logistics as compared to field work

5) They are a galliform bird with good genetic annotation through the chicken genome and the ptarmigan genome available to our research group through collaboration with Iceland.

6) Their brain is large enough to be well suited for *in situ* hybridisation investigations.

7) The Sv. rock ptarmigan is a wild bird. Therefore unlike other common avian models its photoperiodic responses have not been selectively influenced through the domestication process.

The physiological parameters measured in previous studies are downstream of changes in how the brain integrates the peripheral input from the body. A mechanistic understanding underpinning these changes have not been investigated. This thesis aims to examine the effect of photoperiod (PP) on central gene expression within the context of seasonal physiology. Specifically, the overarching goal is to describe the relative mRNA expression levels of the feeding related peptides AgRP, NPY and POMC in the medio basal hypothalamus under different photoperiods and correlate their abundance with longitudinal measurements of physiology and behaviour. This goal is here broken down into four major aims:

1) Characterize the impact of PP on body mass, voluntary food intake and activity.

2) Characterize the impact of PP on Dio2 expression in the medio basal hypothalamus.

3) Characterize the impact of PP on the feeding peptides AgRP, NPY and POMC in the medio basal hypothalamus.

4) Correlate gene expression data to physiological and behavioural data.

2 Material and methods

2.1.1 Experimental animals

Captive bred Svalbard ptarmigan were hatched at the University of Tromsø (69° 39´N, 18° 57´E) between 24.06.17 and 02.08.17. Clutches were maintained either outside on the ground, outside in cages or inside until a body weight of 500g (indicating robust condition) was reached. Twenty-nine experimental birds (16 males and 13 females) were transferred to 5 isolated chambers in a light and temperature controlled lab and placed in cages (1.5m x 0.5m) in order of alternating sex (See appendix for details). *Ad libitum* access to food (standardized protein food; Norgesfor, Ref. No.:OK 2400 070316) and water was provided throughout the experiment. Average room temperature was 6^{o}C and it never exceeded 8^{o}C. Animals where kept in accordance with EU directives under licence provided by the Norwegian Food Safety Authority (Mattilsynet, FOTS7971).

2.1.2 Experimental setup

From five weeks prior to the experiment all birds were kept under DD (0 hours of light). At the start of the experiment (day 0) 5 individuals were sampled as a control group (**Figure 15**). One group of n = 9 animals was transferred to 24 hours of light (LL), one group of n = 9 was exposed to a simulated natural PP with an increase in daylength (NP) following progression of civil twilight on- and offset in Svalbard. One group of n = 6 remained in DD until the end of the experiment. Four individuals were sampled from the LL group after 38 hours of continuous light to investigate acute changes in response to a first long day. Four individuals were sampled from the NP group as they reached LD 12:12. After 9 weeks into the experiment all groups were sampled as shown in (**Figure 15**). During the experiment all birds where sampled at the same time of day to avoid daily differences seen in gene expression of genes of interest. Because a limited number of dissections could be performed within this period the DD group was sampled 24 hours after the LL and NP group.

2.1.3 Activity

Locomotor activity of 29 experimental birds was continuously recorded by passive infrared detection (method outlined in (Appenroth, 2016)) Data was collected using an Actimetrics CL200 USB interface coupled to a ClockLab acquisition package (Version 2.61) running on a PC laptop recording movements detected per minute.

2.1.4 Body mass

Individual body mass (BM) of a subset of birds was monitored once a week in the period from hatching to 16 weeks prior to the experiment. From 16 weeks before the experiment to the end of the experiment body weight was recorded every 1-2 weeks.

2.1.5 Food intake

From 1 week prior to the experiment daily voluntary food intake (VFI) from at least two males and two females of average weight was recorded in each group. To prevent spillage a metal grid was placed on top of the food containers. However, some individuals still succeeded in spilling their food, which was noted on a daily basis. For the sake of consistency and hygiene the spilled food on the tray underneath the bird's cage was not put back into the food bowl.

2.1.6 Collection of samples

2.1.6.1 Tools

Dissections were performed using one large straight scissor and a small bent scissor, one spoon, blunt - nosed thumb forceps, a metal block equilibrated to -80ºC, aluminium foil, gloves and RNase-away. All metal tools where autoclaved before use.

2.1.6.2 Procedure

Birds were euthanized in accordance with guidelines and licences (EU directive, FOTS7971). The brain was rapidly removed as follows: After decapitation the skin was pulled from the neck over the birds' eyes. Remaining neck muscles were cut off with the large straight scissor to expose the back of the skull with the *Foramen magnum*. With the smaller bent scissor I followed the curvature of the skull, with only the part of the scissors outside the skull moving to avoid damage to the brain. Halfway, the scissors were extracted and the same procedure was performed on the other side of the skull. The top of the skull was carefully lifted, exposing the pineal gland sticking to the meninges and carefully removed, thus exposing the brain. A spatula was inserted rostrally to lift the brain so that the strong nerve fibers of the optic chiasm could be cut with the small bent scissors. The brain was further separated from the brainstem using a spoon and scooped out. The brain (often without the cerebellum) was transferred onto a sheet of aluminium foil with the ventral side pointing up. The aluminium foil was placed on top of an aluminium block equilibrated to -80ºC. After the brain was slowly frozen through (can be observed by its colour turning from pink to white), the aluminium block was placed in an ultrafreezer (-80ºC) for storage. The period between death of the animal and freezing of the brain was always under 10 minutes.

2.1.7 Record of physiological processes

Throughout the experiment signs of moult and reproductivity was noted. At each endpoint, the birds where scored from 1-4, accordingly:

1: the whole bird was white (winter phenotype).

2 – the bird had started to moult and some brown feathers on the head and back could be seen.

3 – the head and back were more brown than white.

4 – the whole bird was brown (summer phenotype).

2.1.8 *Primer design*

Since the Svalbard ptarmigan genome is not sequenced, data from Icelandic rock ptarmigan (Lagopus muta) and Swedish willow ptarmigan (Lagopus lagopus) were combined to find regions of high conservation. Sequence data for the genes of interest were retrieved from the chicken genome (ensembl web resource). Following a BLAST (basic local alignment search tool) conserved sequences were identified in the Icelandic rock ptarmigan genome. Due to the poor coverage of the Icelandic rock ptarmigan genome the Willow ptarmigan or Japanese quail genome were used in regions with an unknown sequence Sequences of interest were aligned with Willow ptarmigan, Japanese quail, and chicken sequences using the program Ape to identify conserved regions. Primers (**Table 1**) were designed by copying conserved regions into word and "manually" searching for suitable primers. Parameters for primer suitability were a length of roughly 18 bp, no repetitiveness, unique binding specificity to the region of interest, and an end with a C or G clamp because of stronger hydrogen binding between the C and G compared with A and T. Primers where tested for specificity with the primer BLAST function (NCBI web resource).

Table 1 Primers for genes of interest. Species indicates source of genome used for primer design. Direction (forward or reverse), sequence, optimum temperature for annealing (Tm), and predicted amplicon size in base pairs (bp) are given.

Gene	Species	Forward/reverse	Sequence (5´to3´)	Tm (°C)	Amplicons (bp)
AgRP	Coturnix japonica	Forward	ACCATGCTGAACGCGCTG	58	464
AgRP	Lagopus muta	Reverse	TAGTTCTTGCCGCATGGG	58	464
NPY	Lagopus lagopus	Forward	TGTCGGTGCTGACTTTCG	62	370
NPY	Lagopus lagopus	Reverse	CAATGGCTGCATGCACTGG	62	370
POMC	Lagopus muta	Forward	AGAGCATCCGCAAGTACG	62	503
POMC	Lagopus muta	Reverse	GAACAGAGTCATCAGCGG	62	503

2.1.9 Riboprobe production

Svalbard ptarmigan RNA was extracted from the hypothalamic area using the RNeasy plus universal kit™ (Qiagen). Quality and concentration were assessed by nanodrop (Thermo Scientific 2000c). To convert RNA to cDNA a High-Capacity RNA-to-cDNA Kit™ was used (Thermo Fisher Scientific). Buffer, RNA, enzyme, and water were added in accordance with manufacturer`s instructions. For all samples an equal total volume and concentration of 2 mg RNA was obtained. The tubes were placed in a thermal cycler PCR machine at 37°C for 1 hour, 95 °C for 5 min and 4 °C until pick up. The obtained cDNA was used as a template for subsequent PCR reactions. PCRs were performed using GoTaq® qPCR system (Promega) with cDNA and the respective primer pairs. The annealing step of PCR was run on a temperature gradient (taqgrad) to find the optimized temperature for the reaction (**Table 2**). The PCR products were resolved by gel electrophoresis and visualised on a UV transilluminator (Syngene Chemi Genius imaging system) to asses if the reaction produced an amplicon of the expected length. This process was repeated several times to find the most efficient primer pair and annealing temperature.

Table 2 Thermal cycler. The thermal cycler program Taqgrad was used to find the optimized temperature for the primers. Step 2-4 repeated 35 times.

Step	Temperature	Duration
1	94 °C	3 min
2	94°C	1 min
3	54-62 °C	1 min
4	72 °C	1 min
5	72 °C	5 min

PCR products were excised from a 1% agarose gel processed using the PureLink® Quick Plasmid Miniprep kit (Invitrogen™) according to the manufacturer's guidelines. The concentration of DNA samples was measured using a Nanodrop (Thermo Scientific 2000c) and varied from 2.5-28.4 ng/µl. The DNA was subsequently ligated into the cloning vector (pGEM®-T Easy, Promega) by adding 3 µl of the PCR product, 5 µl buffer, 1 µl vector and 1 µl ligase. The ligation lasted for 1 hour at room temperature. Ligated plasmids were then transformed into DH5α competent cells (*Esherichia coli*). Vectors containing genes of interest were heat shock transferred to the bacteria and was then further kept under favourable conditions for growth in an environment with ampicillin. After one hour at 37 °C in a shaking incubator the bacteria containing vectors were plated on plates containing ampicillin and was incubated over night at 37 °C.

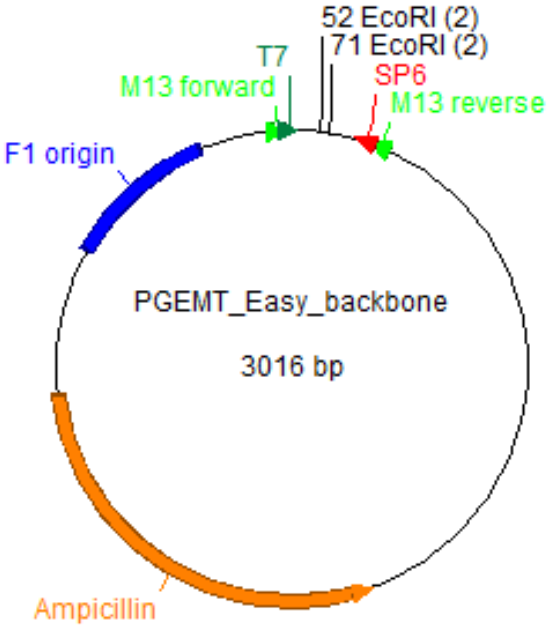

Figure 13 The P-GEM-T easy vector. Illustration of backbone illustrated with the most important features of the vector. The region coding for different functions in the backbone is highlighted as follows: antibiotic resistance to ampicillin (ampicillin), replication start site (F1 origin), promotor site for the M13 forward promotor (M13forward), promotor site for T7 (T7), the digestion site for EcoRI (EcoRI), promotor site for SP6 (SP6), and promotor site for the M13 reverse promotor (M13reverse). The insert would be in the region between the promotors T7 and SP6.

Single colonies were picked from the agar plates and cultured in 4 ml of LB broth supplemented with ampicillin (100 mg/l broth) in a ventilated falcon tube. The tubes where placed in a shaking incubator (225 rpm) at 37 °C overnight. The following morning plasmid DNA was isolated from the bacteria using PureLink® Quick Plasmid Miniprep kit (Invitrogen™) according to manufacturer's instructions. The concentration and purity of the plasmid DNA were determined with a Nanodrop. To determine the length of plasmid inserts the vectors were digested with the restriction enzyme EcoRI. The digested product was resolved on an 1 % agarose (Sigma, A2576) gel, at 70 volts for 1 hr, to visualise the length of the vector and the insert. Plasmid samples with inserts of the expected length were prepared for a Big Dye Reaction (see **Table 3** and **Table 4**) and sent to the in-house sequencing department for sequencing analysis.

Table 3 Big Dye reaction. Reagents and volume needed for the Big Dye reaction.

Reagents:	Volume (µl)
M13 R	0.5
Big Dye	0.5
Buffer	3
Template	x µl = 100 ng
H_2O	Make up to 20µl final volume

Table 4 Big Dye thermal cycler program. Parameters used in the Big Dye reaction. Step 2-3 repeated 40 times.

Step	Temperature (^oC)	Time
1	96	5 min
2	96	10 sec
3	50	5 sec
4	60	4 min

Suitable plasmids were re-transformed and cultured at 200ml volume for a Maxiprep (Qiagen,) purification. The plasmids were re-confirmed by sequencing before the vector was linearized for radioactive *in situ* hybridization use.

2.1.10 Tissue sections

The experimental brains where moved from the -80 ºC freezer to a cryostat (Leica®) set to -20 °C with a microtome. The brain was examined, and abnormalities in shape was noted. Further pre-cooled tissue tek was applied to the brain holder and the brain was carefully placed with the caudal end onto the holder. The tissue tek solidified (turned white) and the brain was properly attached to the holder before the whole brain was embedded in tissue tek. When the whole brain was embedded and the tissuetek had solidified, the brain holder was mounted firmly into the microtome with the ventral side upwards (**Figure 14**). Further the microtome was used to cut 20 µm thick cross-sections of the frozen experimental brains in the region that covers the mediobasal hypothalamus. Sections where kept from where the optic chiasm disappeared and the third ventricle (3V) was prominent. One series consisted of 8 microscopic slides with 3 sections per slide. Around 6 series where collected for all experimental birds. The orientation of the region of interest was centred towards each other to optimize the further processes in the ISH.

Figure 14 Cryostat with mounted ptarmigan brain. Sections of 20 µm were obtained in a cryostat set to -20 ºC.

2.1.11 *In situ* hybridisation (ISH)

2.1.11.1 Linearization

Vector inserts were linearized by adding nuclease free water, template, BSA, buffer and an appropriate restriction enzyme together in a final volume of 100 µl. The digestion was performed on a heated block keeping 37 ºC for 3-4. After this 5 µl were loaded on a 1 % agarose gel to check if the digestion has been completed. If so, 100 µl phenol/chloroform were added to digested mix, vortexed and centrifuged at 13 000 rpm for 5 min. The sample is thus separated into two phases, of which the upper phase (roughly 85 µl) is pipetted into a new tube, to which 5 µl of 5 M NaCl are added. This catalyzes precipitation

after which 250 µl 100 % EtOH from the freezer were added before the tubes were vortexed and centrifuged at 13 000 rpm for 25 min.

The pellet is then clearly visible and the supernatant is carefully removed with a pipet before adding 300 µl 70 % EtOH and centrifugation at 13 000 rpm for 5 min. Again, EtOH is removed with the pipet without disturbing the pellet as far as possible. Tubes are then covered with a piece of paper to avoid contamination, and air dried until all EtOH has evaporated (ca. 5-10 min). The pellet is resuspended with 15 µl nuclease free water. A Nanodrop was used to determine DNA concentration.

2.1.11.2 Day 0 - Riboprobe synthesis

In order the following items were added for transcription: X µl DEPC treated water (depending on DNA concentration Y µl DNA should yield 1 µg/ µl) ,5 µl 5x Transcription buffer, Y µl DNA template, 3 µl NTP mix (1:1 mix of 10 mM rCTP, rGTP, rATP), 2 µl 0.1 M Dithiothreitol (DTT), 1 µl Rnase block 1, 4 µl ^{35}S-UTP, 1 µl T7 or SP6 stock (depending on probe – see **Table 5**) (Riboprobe® Combination Systems, Promega) in a total volume of 25 µl. The mixture was vortexed, spun down and incubated at 37 °C for 1-1.5 hr.

Table 5 Transcription details for all probes. Listed are the probe and its respective transcription factor.

Probe	**Transcription factor**
AgRP AS	T7
AgRP S	SP6
NPY AS	SP6
NPY S	T7
POMC AS	SP6
POMC S	T7

To get rid of excess nucleases not incorporated in the synthesized RNA 2 µl DNase were added and incubated with the Transcript for another 30 min at 37 °C. During this incubation, DEPC-H_2O Chromaspin 50 columns were prepared by resuspending the gel and spinning the columns at 3000 rpm for 1 minute according to manufacturer´s recommendation.

The probe volume of 27 µl was made up with 23 µl of DEPC treated water to a total volume of 50 µl. Tubes were vortexed and 1 µl of the mixture was added to 100 µl DEPC treated water and run through a Chromaspin 50 column. Of this 1 µl is added to 4 ml of scintillant and vortexed to represent total counts before it is rinsed through the chromaspin 50 column.

Liquid scintillation counting (LSC) is the method here used to measure radioactivity. The radioactive material is added to a liquid that react to the radioactivity by emitting photons. The photons emitted is then measured in a scintillation counter.

The probe was pipetted into the Chromaspin column and spun at 3 000 rpm for 2 minutes. Of this eluate 1 µl is added to 100 µl of water. After vortexing 1 µl of this is added to 4 ml of scintillant and vortexed again. This sample represents the incorporation count, which is usually 25-70 % of the total counts. Comparing total counts and incorporated counts indicates how much of the radioactive ^{35}S-UTP is incorporated into the synthesised RNA. Probes can be stored at 4°C for the ISH the following day.

Additional solutions can be prepared for the next day: 4 % paraformaldehyde (PFA), 0.1M triethanolamine (TEA):

A 4 % paraformaldehyde solution was prepared by dissolving 12 g PFA (P 6148, Sigma-Aldrich®) in 150 ml DEPC-H_2O in a baked beaker. It is essential to work under a fume hood as this solution is heated to 70°C under constant stirring. Just before the solution reaches the target temperature, 1-2 drops of 10 N NaOH are slowly added until the solution has become clear. This concentrate is dissolved 1:1 with 0.2 M DEPC-treated phosphate buffer (PB) (see appendix for details). The solution is stored at 4 °C until used the next day.

To prepare a 0.1 M Triethanolamine (TEA) (T1502, Sigma-Aldrich®) solution 1.5 ml 10 N NaOH were added to 5.57 g TEA in a baked beaker before 300 ml DEPC-H2O were added.

2.1.11.3 Day 1 – *In situ* hybridisation

Prior to fixation microscopic slides with sections from the area of interest were warmed from -80°C to -20°C and placed in a rack inside a stainless-steel tank (SS tank). Slides were rapidly covered with 4 % PFA at 4 °C for 20 minutes for fixation. The slides were then washed 2 x 5 min in 0.1 M PB and then immersed in 300 ml 0.1 M TEA for 2 min. Just before the 2 minutes were up, 750 µl of acetic anhydride (AA) were added to an empty SS tank. After 2 min the 0.1 M TEA solution from the rack was poured onto the AA in the fresh SS tank, quickly stirred and slides were again immersed in TEA/AA for 10 min. This was followed by another wash of 2 x 2 min with 0.1 M PB.

The slides were then dehydrated at room temperature (RT) by going through a series of 3 min washes with 50 % EtOH, 70 % EtOH, 95 % EtOH, and 100 % EtOH. After the last wash, the rack was placed in a vacuum chamber for 60 minutes or until all traces of EtOH had evaporated.

During the evaporation a probe mixture was prepared by adding tRNA, 1 M DTT and DEPC-H_2O in a final volume of 70 µl (see appendix for details). Already prepared hybridization buffer (see appendix for details) was added to the probe mixture in a total volume of 350 µl.

For hybridization slides were covered with 70-75 µl of hybridization mixture, covered with coverslips in humidity chambers inside a hybridization oven overnight at 56°C.

2.1.11.4 Day 2- *In situ* hybridisation

The slides were washed 3 x 5 min in 4 x saline-sodium citrate (SSC) and placed in a SS tank with RNase solution (30 ml 5M NaCl, 3 ml 1M TRIS (pH 8) 0,6 ml 0.5 M EDTA and add nuclease free water to make it 300 ml). To this 0,6 ml RNase A were added and slides were incubated for 30 min at 37 °C.

Stringency washes were performed with 2 x 5 min 2x SSC with 0.1 % DTT. 10 min wash with 1 x SSC and 0.1 % DTT, and 10 min 0.5 x SSC with and 0.1 % DTT . Following this slides were incubated for

30 min in 0.1 x SSC with 1 % DTT at 60ºC. Finally slides were rinsed with 0.1 x SSC with 0.1 % ml DTT at RT.

Dehydration was again achieved by 3 min washes each with 50 %, 70 %, 96 % and 1 minute 100 % EtOH and finalized with a drying period of 60 min in a vacuum chamber.

Slides were then placed in a film cassette with the sections exposed to an x-ray film (Carestream® Kodak® BioMax® MR film, Sigma-Aldrich®) under red light in a dark room. The cassette was closed, wrapped in aluminium foil, and put in a cupboard for up to 17 days before the films were developed.

2.1.11.5 Film development

For film development in a dark room the X-ray films were immersed in a film tray with developer (Carestream® Kodak® autoradiography GBX developer/replenisher, Sigma-Aldrich®) for 3 min, rinsed for 10 seconds in tap water and then immersed in a fixer solution (Carestream® Kodak® autoradiography GBX fixer/replenisher, Sigma-Aldrich®) for 3 minutes. The film was then cleared under running tap water for 10 min and air dried in the dark room for at least 1 hour.

2.1.12 Preparation for image analysis

Autoradiographs were scanned (Epson™ perfection v800) together with an industrial optical density calibration ladder (Stouffer Industries, T2115).

2.1.13 Image analysis

Where mRNA of interest was expressed on brain sections, radioactive probe was bound to the tissue during hybridization. The strength of the radioactive signal then causes a directly correlated exposure signal on the X-ray films, allowing us to measure relative mRNA expression as optical density values. All films were analyzed with the free ware Image J. Optical density was calibrated for each autoradiograph and optical density of the areas of interest was recorded by thresholding measurements to the exposed areas of the brain sections. For each bird one brain section was measured. A threshold was adjusted for each section so the edge of the signal was still visible, thus accounting for the typical "spread" of a radioactive signal. The chosen area was measured and a mean grey value calculated. Only the mediobasal hypothalamus/ARC, an area documented to contain central appetite regulators, was analyzed. All measurements were taken blind and data were ordered in treatment groups afterwards. Where values did not pass the Shapiro-Wilk normality test ($P<0.05$), data were transformed to a log scale to correct for this. The test was re-run, and the transform y=log (mean grey value) passed the normality test. Assumptions for Tukey's multiple comparison test were thus fulfilled. P-values are indicated on graphs showing optical density.

2.1.14 Data Analysis

To handle and sort raw data Microsoft Excel™ was used. All graphs and statistical analysis were made with the use of the software GraphPad prism 7™. Significant outliers were identified and excluded before a Shapiro-Wilk normality test was performed to be able to meet the assumption of a normal distribution in an ANOVA. If the test was passed, either a Tukey's post hoc test was used for multiple comparisons between all groups or a Dunnett`s multiple comparison test was used to compare the DDcontrol with the other groups.

2.1.15 Activity data analysis

All bird's activity data were recorded and saved as a file with beam breaks every minute. The start and stop point for all birds were standardised and the activity per minute recordings where saved as text files. To reduce experimental noise the activity was binned into total beam breaks every 20 minutes. Due to variability in equipment sensitivity and individual activity levels of the birds the activity was divided by the 99 percentiles of these binned data for each bird and then saved as a new text file. The text file was then imported into the plugin Actogram J in the program ImageJ to create an actogram. The minimum value was set to 0 and the maximum value to 1, where 0 is no activity and 1 is the 99 percentiles value for that bird. In this way all actograms were normalised and comparable.

The normalised 24-hour activity was calculated for all birds, except the FLD, by a mean of 4 consecutive days prior to euthanasia. The activity in the FLD group were calculated in the first 24 hours this group was exposed to LL. The sum of this 24h activity was divided by the 99 percentiles for each bird. After the data were transformed, a 1way ANOVA was used to test for differences within the three end groups.

2.1.16 Voluntary food intake data

The VFI data are presented as the mean VFI for each bird within each PP group prior to euthanasia. For the DDc all experimental groups where on the same PP, and measurements for 9 birds were included. The mean was taken from the VFI measurements 8 days prior to euthanasia. To have a comparable amount of time between each VFI measurement, 10 hours of DD where included to the time in LL in the FLD group. Mean VFI for the NP12:12 was calculated on food intake 6 days prior to euthanasia. The VFI was consistent for the three birds measured in the NP12:12 group, even though they experienced an increase in day length. In the end point groups NP (n=4), LL (n=5) and DD (n=4), a mean of VFI for each bird from 10 days prior to euthanasia was calculated. Due to sickness, one bird in the DD group was excluded from the analysis (n=3). To test effect of the photoperiodic treatment on VFI a 1way ANOVA was used.

2.1.17 Linear regression

Mean BM of each photoperiodic group was plotted against mean VFI over time. A linear regression was drawn in GraphPad Prism 7™. The same was done for mean BM against activity, optical density measurements of Dio2 against NPY, and optical density measurements of AgRP against BM.

3 Results

3.1 Experimental design

The photoperiodic signal entrains seasonal physiological changes in the Sv. rock ptarmigan. We designed a study to characterize the effect of three different PPs (**Figure 15**). All animals were kept under DD for 5 weeks and at the beginning of the experiment 5 animals were sampled in (DDc). One experimental group (DD, n = 6) was kept under constant darkness (**Figure 15**). One group (LL, n = 5) was abruptly shifted from DD to LL. To detect central responses to this change, a "First Long Day" group (FLD, n = 4) was sampled 38 hrhr after lights were turned on. The last group was kept under a simulated natural PP (NP, n = 9) mimicking civil twilight on- and offset on Svalbard. When the NP group reached an equinoctial PP of 12 light and 12 hr darkness (NP 12:12), a subset of 4 birds was sampled. The final collection for the DD, LL and NP groups came at 10 weeks.

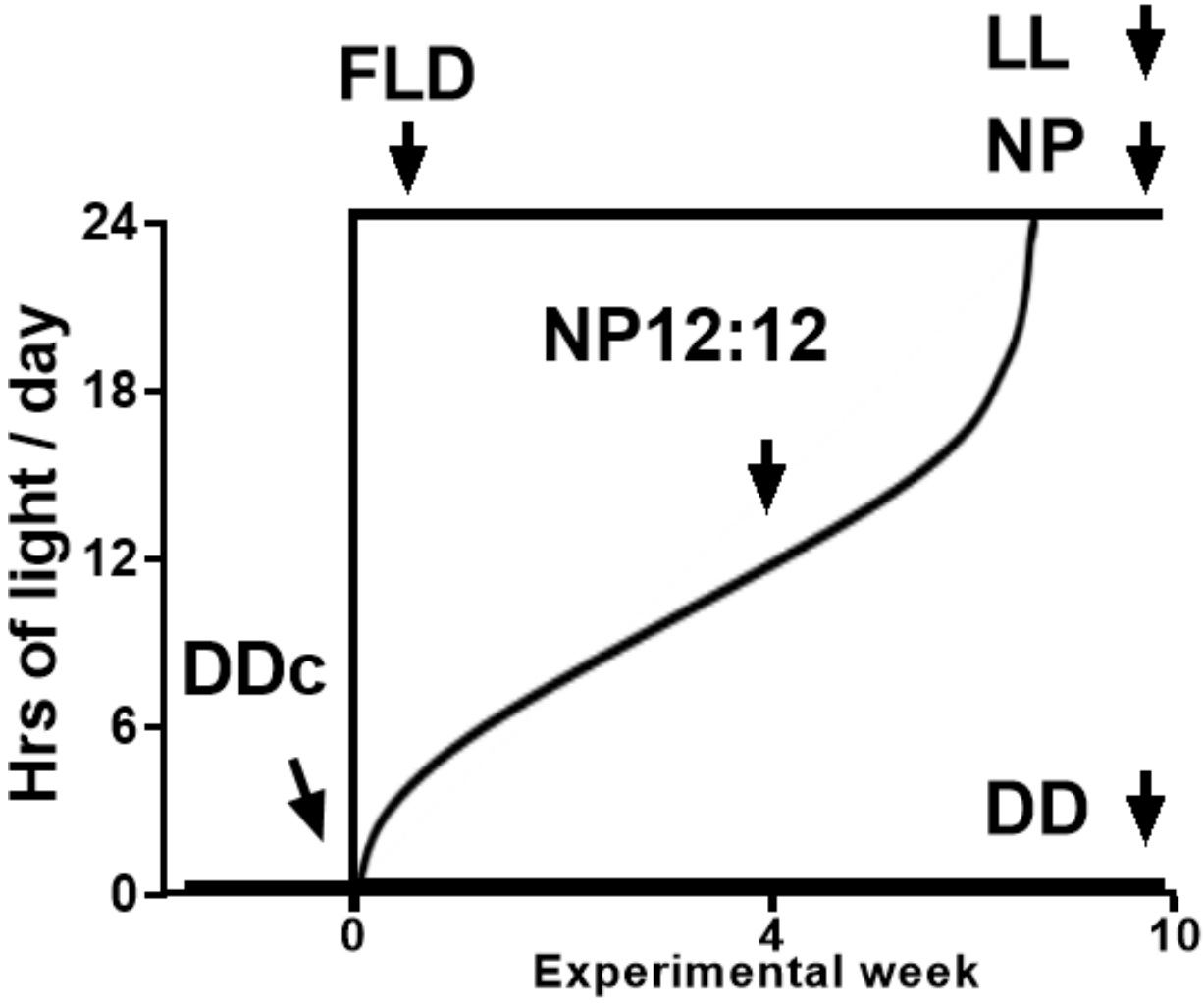

Figure 15 Three groups of Svalbard rock ptarmigan were exposed to different PPs. All birds were kept in constant darkness (DD) for 5 weeks prior to the start of the experiment (0). A control group (DDc, n = 5) was sampled on day 0 and one group remained in darkness (DD, n = 4). One group received constant light (LL, n = 9), one group was exposed to a gradual increase in daylength, simulating natural PP (NP, n = 9) on Svalbard. In the LL group a subset was sampled 38 hr after lights where turned on (first long day, FLD, n = 4). In the NP group a subset of birds was sampled after 4 weeks when the simulated natural PP reached 12 hr of light and 12 hr of darkness (NP12:12, n = 4). The endpoint was 10 weeks after the Photoperiodic switch and the LL, NP and DD group were all sampled at the same time of day. Temperature was kept at 4-6 °C.

3.2 Influence of PP on body mass, voluntary food intake and activity

The seasonal changes in Svalbard rock ptarmigan phenotype are driven by PP. Energy deposition, appetite and food intake, and energy expenditure are the three most important components in the energy balance of an organism. We measured the effect of PP (**Figure 15**) on body mass (BM, **Figure 16A, 18D, E and F**), voluntary food intake (VFI, **Figure 16B**, **18 G**, **H** and **I**) and activity (**Figure 16C,18J, K and L**). To demonstrate changes over time, measurements of BM, VFI and activity were recorded throughout the experiment (**Figure 16**), in addition to above mentioned endpoints (**Figure 17**).

3.2.1.1 Body mass

All groups had a similar mean BM at experimental start (P=0.428). In response to Photoperiodic treatment over time the groups separated in their change of BM (**Figure 16**A, **Figure 17D**, **E** and **F**). The group that remained in DD increased their BM on average 100 g (**Figure 17D**, P<0.01) while the LL (**Figure 17E**, P<0.001) and NP (**Figure 17**F, P<0.01) groups decreased BM by an average of 200 g. The FLD group showed no significant difference in BM during the 38 hr LL exposure (**Figure 17E**, ns). The birds under NP12:12 had a BM between the DDc and NP groups (**Figure 17F**), but did not statistically differ from the DDc group.

3.2.1.2 Voluntary food intake

The DD-group slightly increased their VFI after 3 weeks in DD (**Figure 16B**), but this was not statistically different to experimental endpoint after 9 weeks in DD (**Figure 17G**). Sv. rock ptarmigan experiencing an abrupt shift from DD to LL showed an acute and significant decrease in VFI (P<0.01), but after 9 weeks in LL showed an overall increase in VFI compared to their own starting point (**Figure 17H**, P<0.05). The NP group showed a gradual decrease in VFI when exposed to light, but not as pronounced as the LL group (**Figure 16B**, ns).

3.2.1.3 Activity

Activity levels of Sv. rock ptarmigan in DD remained similar throughout the experiment (**Figure 16C**) (**Figure 17**J, **Figure 18**). An immediate response to lights on in the FLD group resulted in an increase in activity (P<0.01; **Figure 17K**, **Figure 19B**). After 9 weeks in LL the birds still maintained an elevated level of activity compared to their activity in DD (P<0.05, **Figure 17K**, **Figure 18**). The birds under NP showed an increase in activity as PP increased and their activity pattern aligned with the on- and offset of light (**Figure 20**). The overall activity in 24hour activity levels when exposed to 12 hr of light (NP 12:12) did not differ statistically from the activity in DD (**Figure 17L**). After exposure to 24 hr of light for one week 24hour activity levels differed from both, their activity in DD (P<0.001) and NP12:12 (**Figure 17L**, P<0.05).

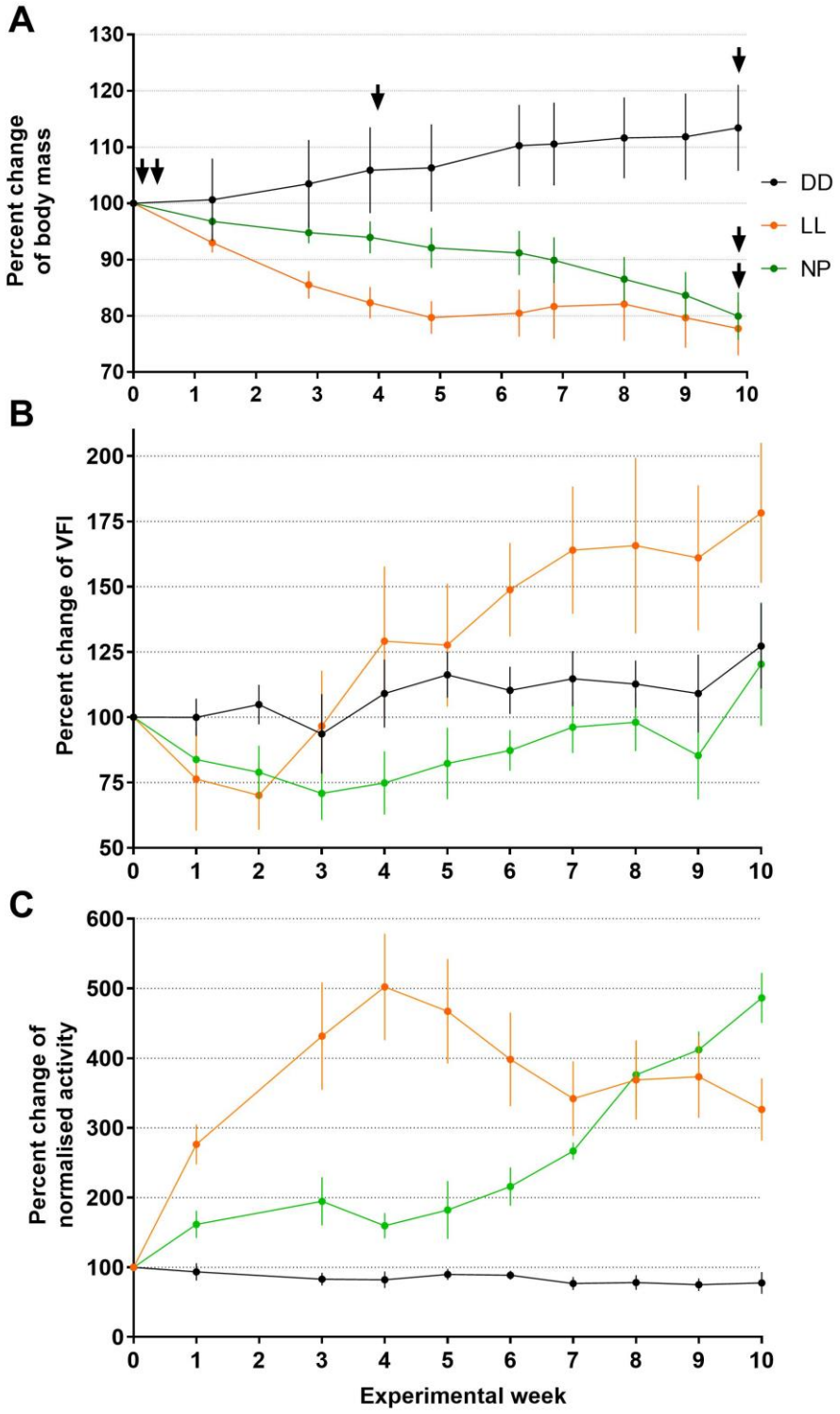

Figure 16 Influence of photoperiod (PP) on body mass (BM), voluntary food intake (VFI) and activity of Svalbard rock ptarmigan. (A) The percental change of BM relative to week 0 (data shown as mean ± SD) for birds kept in constant darkness (DD, n=6), constant light (LL, n=5) and under a natural PP (NP, n=5). Arrows indicate when sub-groups where sampled, from left to right: DDc, FLD, NP12:12, DD, LL and NP. (B) Percental change of a weekly average of voluntary food intake (VFI, mean ± SEM) relative to average VFI 1 week prior to experimental start (DD n=4, LL n=5, NP n=4). (C) Percental change of normalised mean 24 hr activity relative to mean 24 hr activity over 4 days prior to the experiment (mean ± SEM, DD n=6, LL=4, NP n=4). The activity was normalised by dividing by the 99 percentile. DD - black closed circles, LL- orange closed circles, NP- green closed circles.

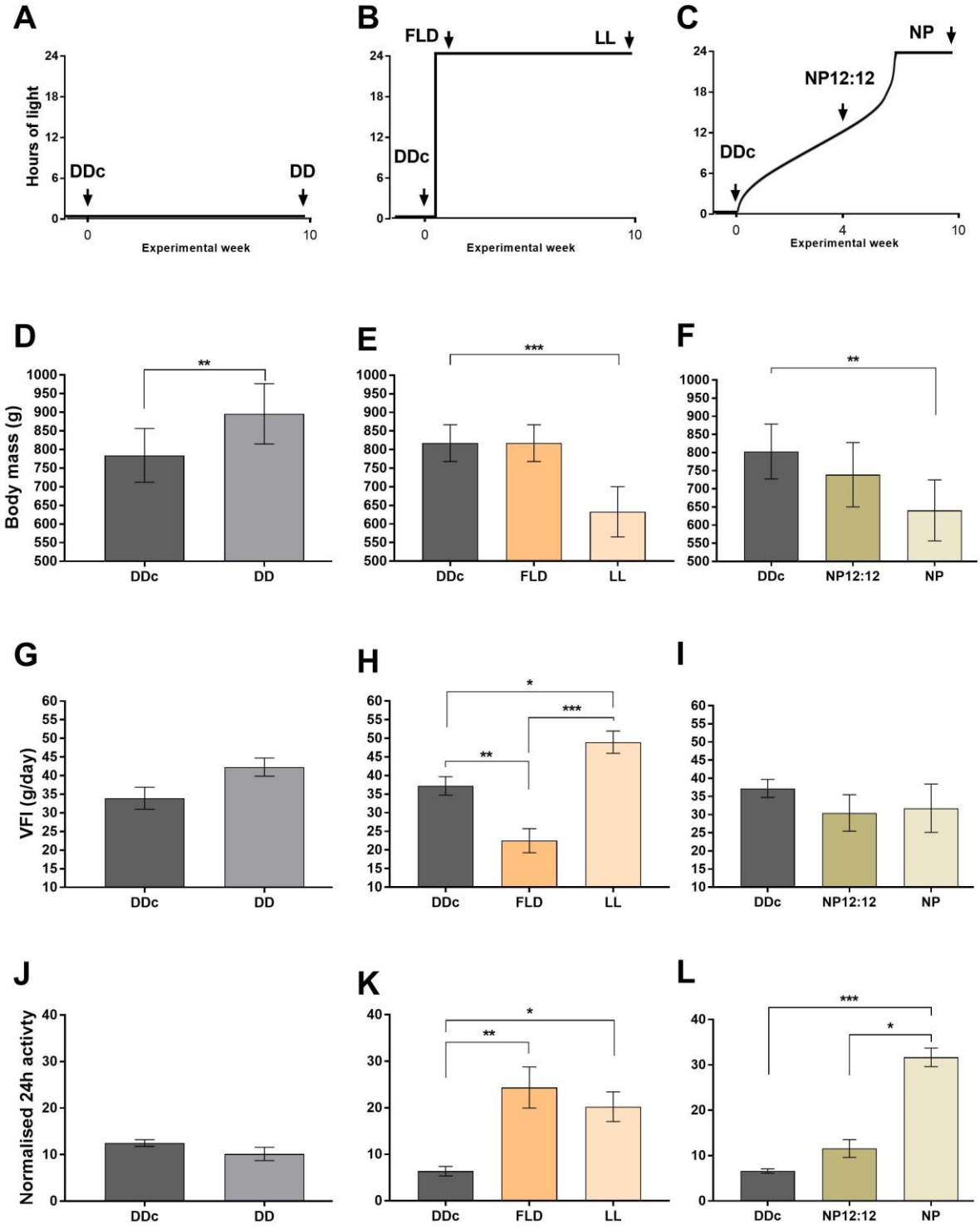

Figure 17 Effect of PP on physiology and behaviour of Svalbard rock ptarmigan (A) Experimental design for the group held in constant darkness (DD), (B) in constant light (LL) and (C) under a natural PP (NP). Each sampling point is indicated with an arrow. (D) Group body mass in g (mean ± SD) for birds under DD (n=6), (E) LL (n=5) and (F) NP (n=5). (G) Group voluntary food intake in g per day (mean ± SEM) under DD (n = 3-4), (H) LL (n=5) and (I) NP(n=3-4). (J) Normalised 24hour activity of 4 days prior to each timepoint (mean ± SEM) under DD (n=6), (K) LL (n=4) and (L) NP (n=4). *P<0.05, **P<0.01, ***P<0.001. A paired t-test was applied to test for differences between two groups. 1way ANOVA post-hoc Tukey`s multiple comparison test was used to test for differences between three groups.

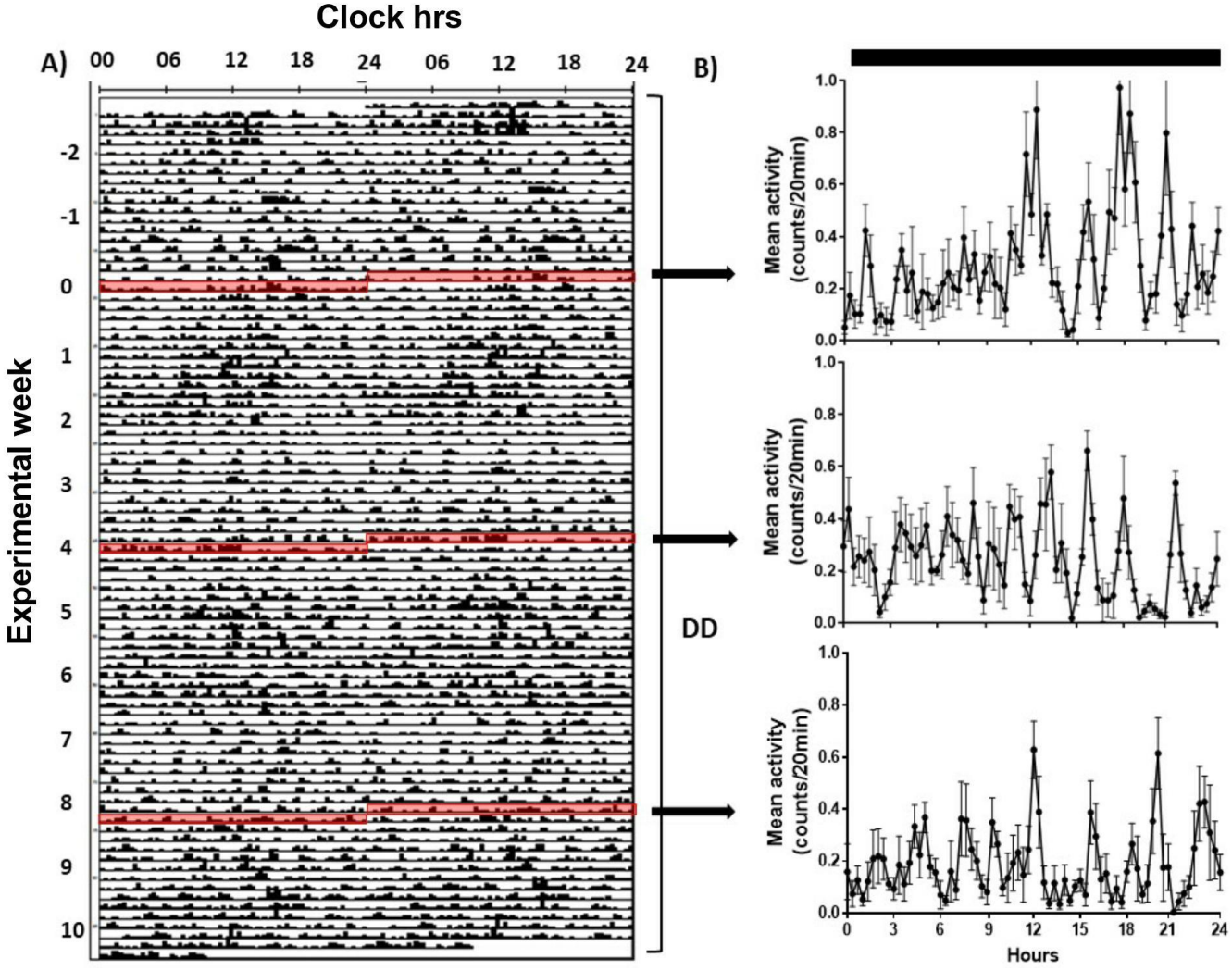

Figure 18 Activity of Svalbard rock ptarmigan in constant darkness. (A) Double plotted actogram of a representative female. Activity is in 20 minutes bins divided by the 99 percentiles and the upper and lower limits ranging from 0 (no activity) and 1 (99 percentiles). The X-axis depicts clock hr and the y-axis experimental week. Each line on the actogram represents 2 days with the second day being repeated in the next line. (B) Group activity (mean ± SEM, n=6) in constant darkness (DD) at three different days (marked in red) during the experiment. Black bar on the top the graph (top) indicate Lights off.

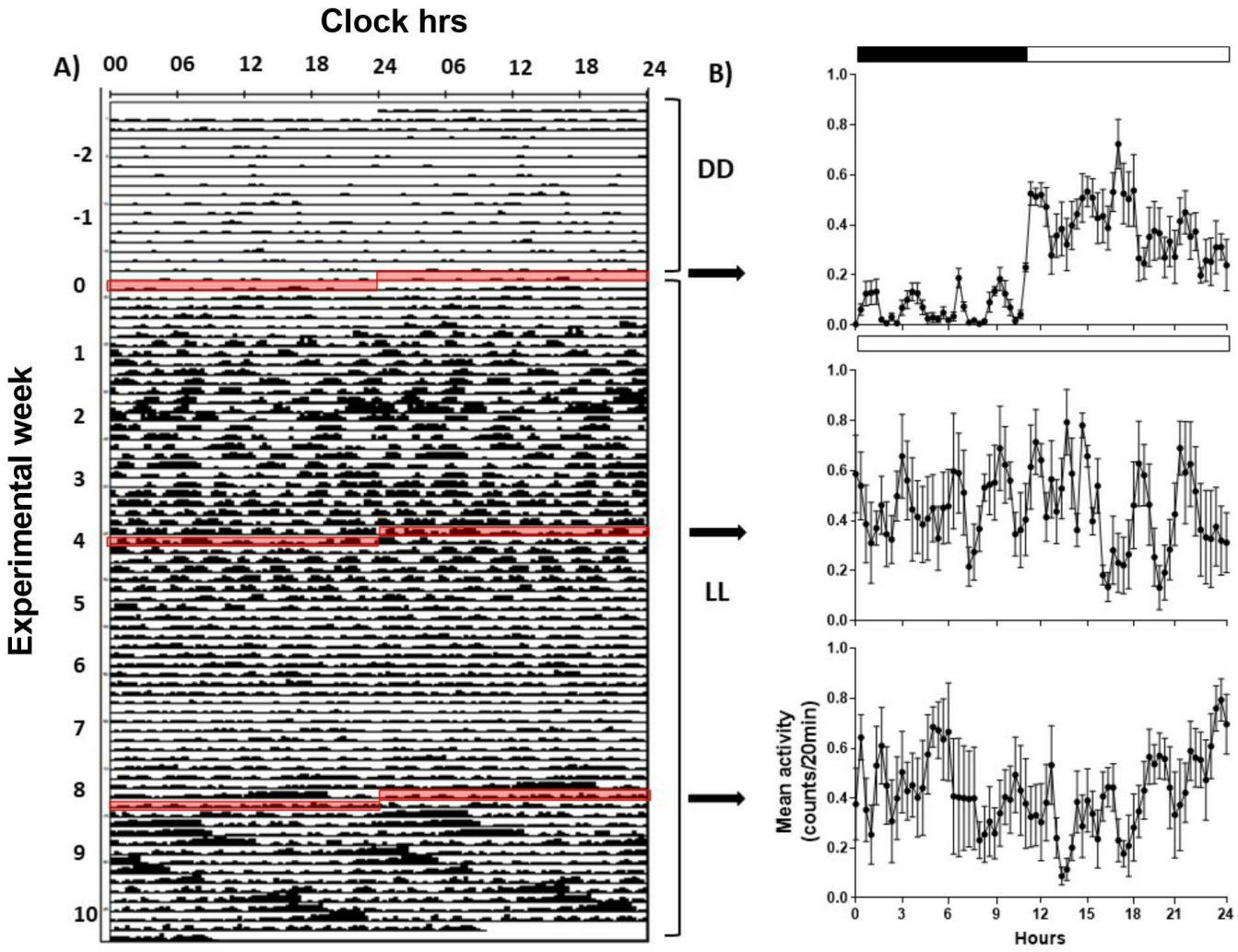

Figure 19 Activity of Svalbard rock ptarmigan in constant light. (A) Double plotted actogram of a representative female. Activity is in 20 minutes bins divided by the 99 percentiles and the upper and lower limits ranging from 0 (no activity) and 1 (99 percentiles). The X-axis depicts clock hr and the y-axis experimental week. Each line on the actogram represents 2 days with the second day being repeated in the next line. (B) Group activity (mean ± SEM, n=6) in constant darkness (DD) at three different days (marked in red) during the experiment. Black bar on the top the graph (top) indicate Lights off.

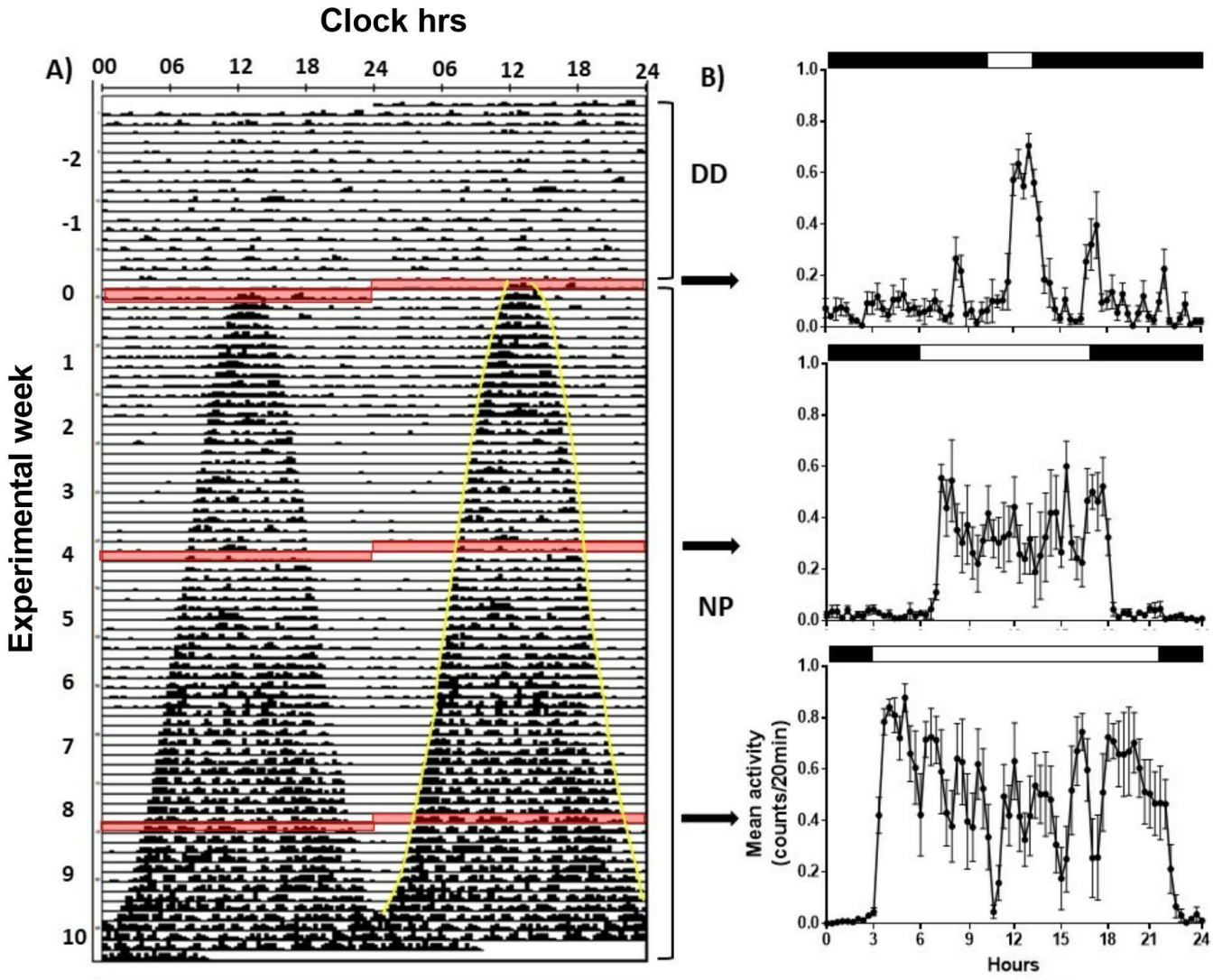

Figure 20 Activity of Svalbard rock ptarmigan under a natural PP. (A) Double plotted actogram of a representative female. Activity is in 20 minutes bins divided by the 99 percentiles and the upper and lower limits ranging from 0 (no activity) and 1 (99 percentiles). The X-axis depicts clock hr and the y-axis experimental week. Each line on the actogram represents 2 days with the second day being repeated in the next line. (B) Group activity (mean ± SEM, n=6) in constant darkness (DD) at three different days (marked in red) during the experiment. Black bar on the top the graph (top) indicate Lights off.

3.3 Relationship between body mass, voluntary food intake and activity

A linear correlation was found between VFI and BM in the DD group (**Figure 21A**, P<0.05), but not in the LL- and NP group (**Figure 21C**, ns and **E**, ns, P=0.058). Linear regression between activity and BM showed a correlation in the birds under NP (**Figure 21F**, P<0.001), but not the birds exposed to LL (**Figure 21D**, ns) and DD (**Figure 21B**, ns).

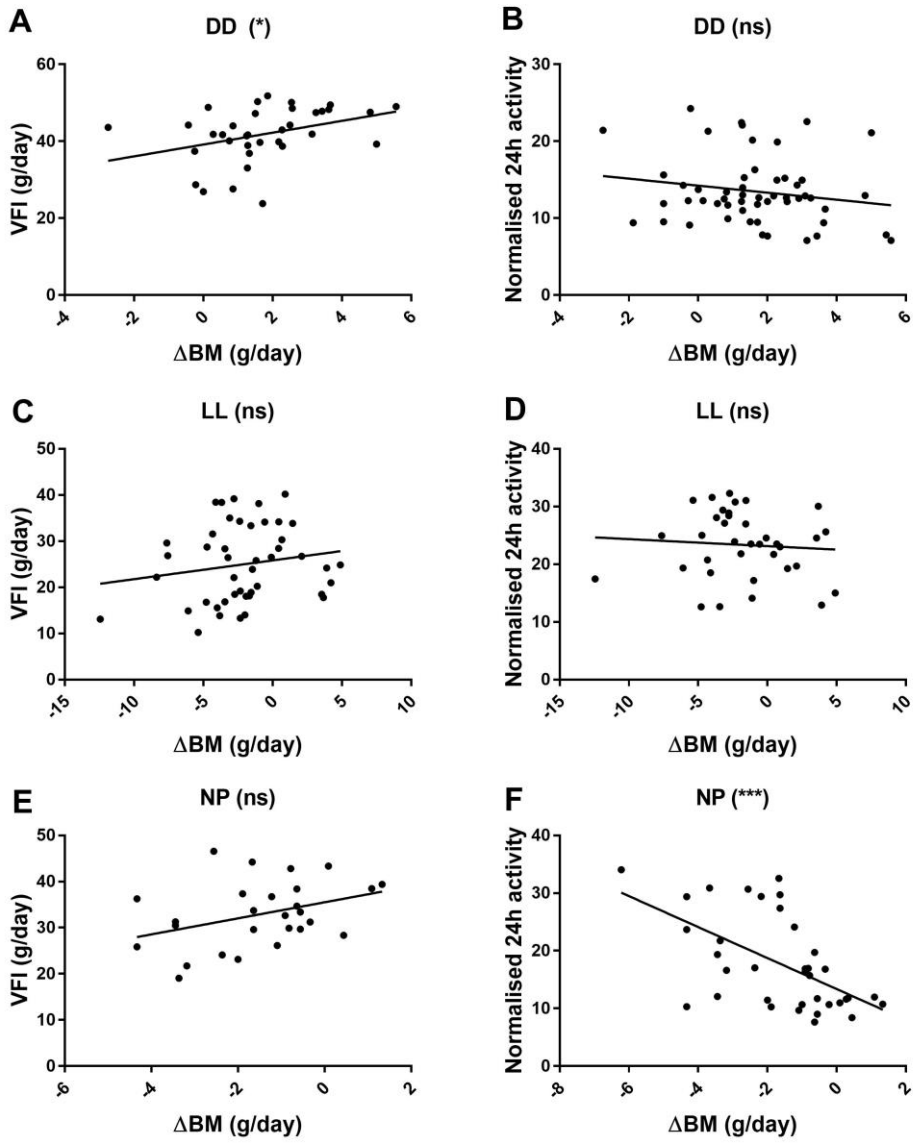

Figure 21 Relationship between body mass (BM), voluntary food intake (VFI) and activity in Svalbard rock ptarmigan kept under different PPs. Changes in individual average voluntary food intake (VFI) (g/day) plotted against individual changes of BM (g/day) and individual 24hour activity plotted against individual changes of BM (g/day) in the three Photoperiodic groups held in constant darkness (DD) (A&B) constant light (LL) (C&D) and under a natural PP (NP) (E&F). The average VFI was calculated from the time between each BM measurement. * P<0.05, ***P<0.001, ns: not significant.

3.4 Physiological processes

Throughout the experiment only the LL group started moulting and egg laying (**Table 6**).

Table 6 Moult score and signs of reproduction. The three PP groups and their respective moult score at the end of the experiment, and the signs of reproduction throughout the experiment. Moult score: 1- white (winter phenotype), 2 – head and back with some brown feathers, 3 – head and back brown, 4 – whole bird brown (summer phenotype)

Photoperiodic group	Moult score at endpoint (1-4)	Onset of moult	Signs of reproduction
DD	1	No	No sign
LL	3 females 2 males	Females: week 4 Males: week 8	Males vocal week 1 First egg laid in week 7
NP	1	No	Males vocal week 8

3.5 Influence of photoperiod on gene expression

The arcuate nucleus is documented to be the central appetite center of the brain and resides within the medio basal hypothalamus. We here document the expression of the central feeding peptides AgRP, NPY and POMC, in addition to the seasonal marker Dio2 within the MBH.

3.5.1.1 Dio2

To investigate the photoperiodic state within the brain of the Sv. Rock ptarmigan Dio2 was used as a seasonal marker. Expression of Dio2 in Sv. rock ptarmigan in DD for 9 weeks was elevated compared the DDc group (**Figure 22A**,$P<0.01$). Only 38 hr of LL caused a significantly increased expression of Dio2 in the FLD group compared to the DDc group (**Figure 22A**, $P<0.001$). The highest expression was found in the group exposed to LL for 9 weeks (**Figure 22A**, $P<0.0001$). Expression of Dio2 in birds kept under NP12:12 was lower than other groups and did not statistically differ from DDc (**Figure 22A**, $P=0.1051$). After 9 weeks under NP Dio2 expression differed from the DDc group (**Figure 22A**, $P<0.01$).

3.5.1.2 AgRP

Expression of AgRP in the three groups exposed to no light (DDc and DD) or a short duration of light (FLD, **Figure 22B**) is low. The groups exposed to more light (NP12:12 and NP and LL endpoints) show an increase in the expression of AgRP (**Figure 22B**). Only the LL group differed significant from the DDc group ($P<0.05$).

3.5.1.3 NPY

All groups showed expression of NPY and expression was elevated in all three end groups compared to DDc (**Figure 22C**, $P<0.05$). The expression was slightly increased in the FLD and the NP12:12 group.

3.5.1.4 POMC

Gene expression of POMC in Sv. rock ptarmigan is not affected by PP (**Figure 22D**).

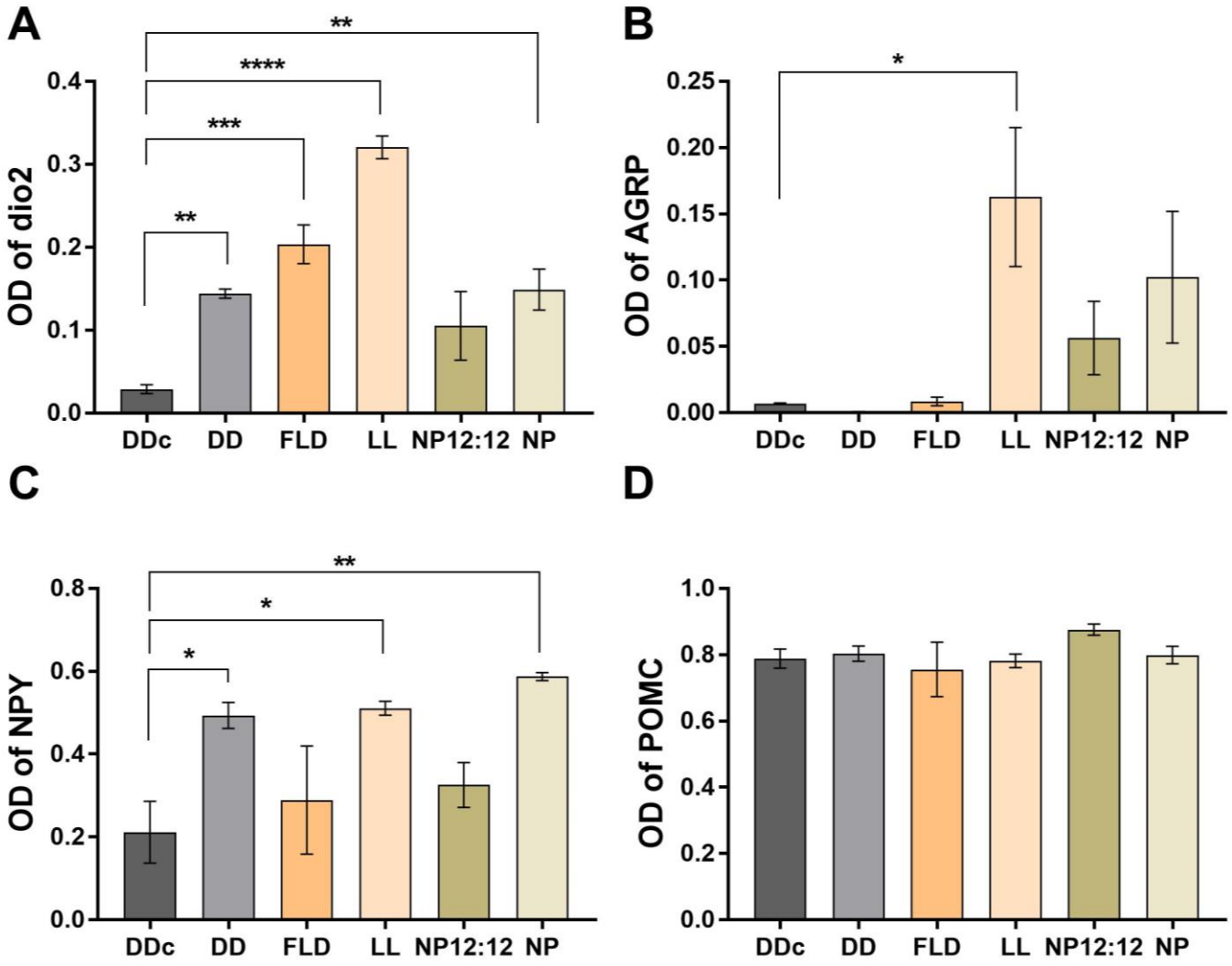

Figure 22 Influence of PP on gene expression in the brain of Svalbard rock ptarmigan. (A) Optical Density (OD) measurements of Dio2 (B) AgRP, (C) NPY and (D) POMC in the mediobasal hypothalamus of the Sv. rock ptarmigan. All data are presented as ± *SEM (n = 4)*. *P<0.05, **P<0.01, ***P<0.001, ****P<0.0001. 1way ANOVA post-hoc Dunnett`s multiple comparisons test was used to detect differences between the DDcontrol (DDc) and the remaining groups. Constant darkness (DD), first long day (FLD), constant light (LL), natural photoperiod 12:12 (NP12:12), natural photoperiod (NP).

3.5.1.5 Autoradiographs

Autoradiographs obtained by radioactive *in situ* hybridization were used to measure optical density (OD) of Dio2, AgRP, NPY and POMC in the Medio basal hypothalamus of the Sv. Rock ptarmigan (**Figure 23**). These measurements allowed us to see how the seasonal status, Dio2, of the bird affected the expression of the central appetite regulators AgRP, NPY and POMC.

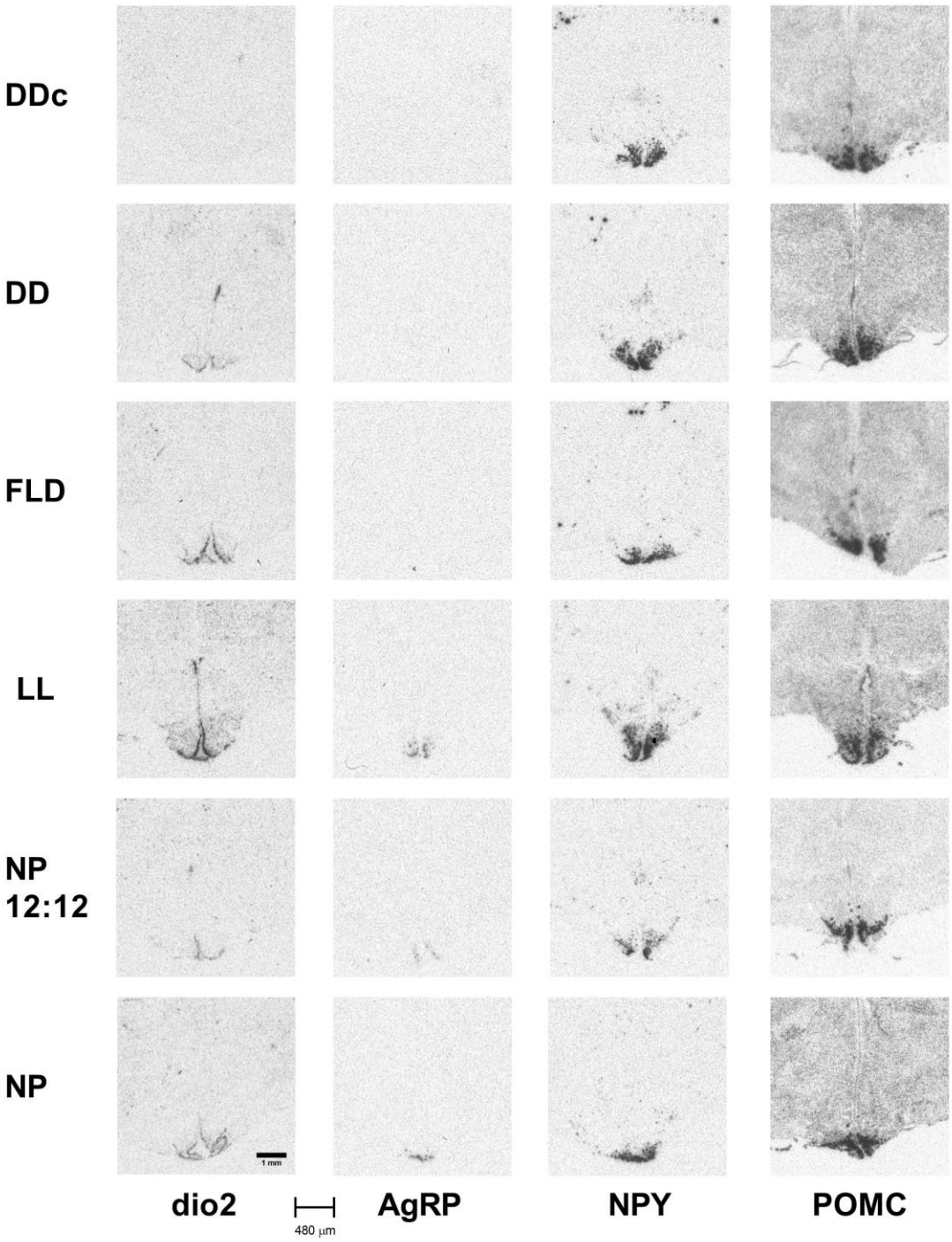

Figure 23 Autoradiographs of gene expression in the Svalbard ptarmigan mediobasal hypothalamus. For each experimental group Dio2, AgRP, NPY and POMC gene expression was determined by radioactive in situ hybridization. One representative individual is shown per group. For each individual bird the sections for AGRP, NPY and POMC are consecutive, while Dio2 is 480 µm anterior to AGRP. All images correspond to scalebar (1mm) shown in autoradiograph for Dio2 in the NP group. Constant darkness control (DDc), constant darkness (DD), first long day (FLD), constant light (LL), natural photoperiod 12:12 (NP12:12), natural photoperiod (NP).

3.5.1.6 Relationship between a seasonal marker and an orexigenic peptide

A correlation between the OD measurements of Dio2 and NPY was found and the relationship is shown as a linear regression in **Figure 24A**, $P<0.01$. Further, an inverse correlation between OD measurements of AgRP and BM was found (**Figure 24B**, $P<0.05$).

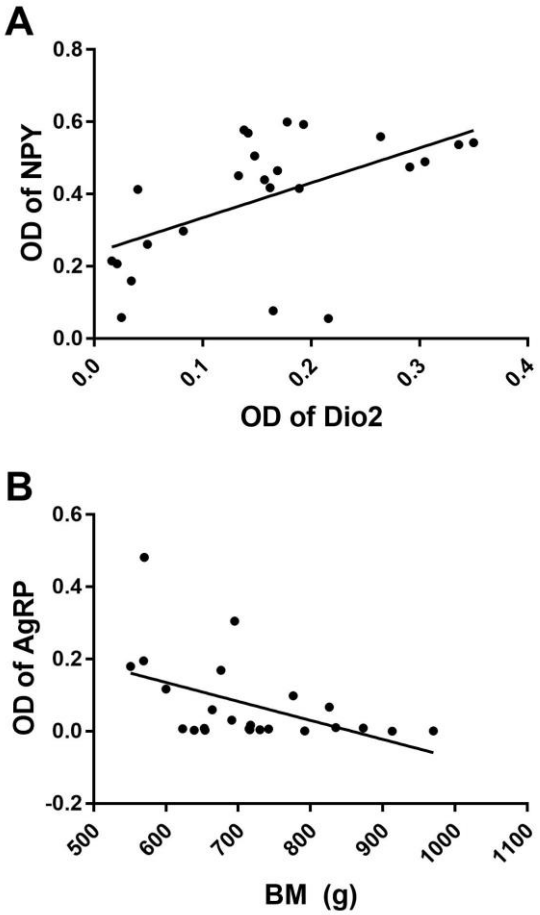

Figure 24 Relationship between Dio2 and NPY, and BM and AgRP. (A) optical density (OD) measurements of NPY plotted against Dio2 ($P<0.01$). (B) Body mass (BM, g) plotted against OD measurements of AgRP ($P<0.05$).

4 Discussion

4.1 Seasonal phenotypic changes are suppressed by darkness and accelerated by light

In the wild the Sv. rock ptarmigan display a seasonal change in phenotype which enhances fitness and survival. In the lab this phenotypic change can be manipulated by controlling PP. Previous work has shown that wild juvenile Sv. rock ptarmigan show a decrease in dissectible fat from October to February. In March and April, a stable amount of dissectible fat is documented. Adult females, but not juveniles increase in amount of dissectible fat in May and June (Mortensen et al., 1983). Similarly, captive Sv. rock ptarmigan under natural photoperiodic conditions show a seasonal fluctuation in BM with a peak in October. Contrary to the gradual decrease of dissectible fat in the wild, the BM of the captive birds stay elevated until February. From February a gradual decline of BM occur until June (Lindgård et al., 1995). Here we use established photoperiodic paradigms to investigate the link between seasonal physiology and the expression of key neural regulators known to control energy balance in the Sv. rock ptarmigan.

In our studies the groups exposed to NP differed in their BM, VFI and activity compared to their start-point. The changes in BM documented in the NP group correlated with an increase in activity (**Figure 21F**), but not with changes in VFI (**Figure 21E**). These results are consistent with previous studies which documented activity to be the main driver for a reduction in BM under NP (Lindgård et al., 1995). The gradual increase in PP is shown in the gradual increase of activity. In week 9, when the NP group reached LL, they show the same peak activity levels as the LL group displayed in experimental week 4 (**Figure 16C**). This indicates that the activity level is not simply passive to the PP but requires 4 weeks to adjust to the new environment.

Groups exposed to LL differed in their BM, VFI and activity compared to their start-point. The abrupt transition from DD to LL caused an acute drop in VFI and increased levels of activity. This change of behaviour is likely a stress response to the dramatic shift in the environment. It is also possible that this effect is a result of a compensatory mechanism attempting to rapidly adjust the phenotype to align a mid-summer PP. The decrease in VFI lasted for 2 weeks (**Figure 16B**) and was accompanied by a sharp fall in BM, which may count in support of either hypothesis. The increase in VFI observed from week 3 and onwards is not reflected in the negative development of BM (**Figure 16A**, **B** and **Figure 21C**). Females started to moult in week 4 and the ingested additional calories were surely reallocated to this energetically demanding process instead of being deposited as fat. Additionally, the first egg was laid in week 7 demonstrating that moult coincided with the initiation of reproduction (**Table 6**). The decrease of activity in week 7 coincided with the onset of nesting behaviour and egg laying observed in the females.

Prolonged exposure to DD results in an increase in body weight in the Sv. rock ptarmigan, a trend to increase VFI, but not activity. There was a correlation between the change in BM and the change in VFI and the increase in VFI is likely to be the main driver for the increased BM (**Figure 21A**). Compared to the LL and NP groups these data also suggest that summer body mass reduction observed in the Sv. Rock ptarmigan requires a long PP.

4.2 The photoperiodic machinery in the MBH is conserved in arctic galliformes

Current theory holds that the increase in Dio2 expression within the tanycytes of the third ventricle increases the conversion from T4 to T3 which in turn induces GnRH secretion to the pars distalis (PD) (Miera et al., 2013). The increase of GnRH induces secretion of LH and FSH from the PD, which stimulates the maturation of reproductive organs (Yoshimura et al., 2003). We here demonstrate that the expression of Dio2 in the MBH is dependent upon the PP and endogenous timing mechanisms of the Sv. rock ptarmigan (**Figure 22A**). The expression of Dio2 did not significantly differ under NP12:12 compared to the DDc, which indicates that LD12:12 is below the critical PP for this species (**Figure 22A**). This is consistent with previous critical PP experiments in willow ptarmigan (*Lagopus lagopus*) which showed a seasonal response to LD14:10, but a higher PP was needed to complete the process of photorefractoriness (Stokkan et al., 1982). The NP end group experienced 1 week of LL and showed significantly higher Dio2 expression than the DDc group. Interestingly these expression levels are comparable to the DD group (**Figure 22A**). As previously documented in the Japanese quail Dio2 was induced by the end of the first long day. This indicates that the photoperiodic machinery in the MBH of the Japanese quail is conserved in the Sv. Rock ptarmigan. The expression of Dio2 continues to increase, reaching a peak in the LL group (**Figure 22A**). The continuation of the increased expression levels is consistent with the physiology and behaviour documented in this group (**Table 6**). Moreover, the DD group had a BM, activity levels and VFI as typical of a winter phenotype, not aligning with the phenotype expected 15 weeks after DD onset in their natural environment. The increase of Dio2 expression documented in the DD group indicates an internal seasonal regulation of Dio2. It appears that the birds became photorefractory to the prolonged darkness, and spontaneously upregulate the expression of this enzyme despite the contradictory light signal. This is a response well characterised in seasonal mammals but is a novel observation in avians (Miera et al., 2013). Since the expression levels where comparable to values in the NP group, this possibility is strengthened.

The elevated expression of Dio2 measured in the FLD group clearly demonstrates the acute impact of lengthening PP on the seasonal physiology of these birds (**Figure 22A**). This may be particularly problematic within the context of global climate change where arctic regions are subjected to accelerated temperature increase (IPPC, 2014). The predicted increased temperature at Svalbard will increase the trophic mismatch between the Sv. Rock ptarmigan internal seasonal timing and the environment. This temporal off-set of fine-tuned adaptations will influence the fitness and survival of the organism. It is therefore arguably essential to investigate the plasticity of the internal seasonal timing machinery to understand the effect of climate change on the Sv. Rock ptarmigan population.

4.3 Regulation of feeding related neuropeptides in the MBH of the Sv. rock ptarmigan

The present study used radioactive in situ hybridisation to quantify specific histological expression of key feeding related neuropeptides. Previous work has demonstrated that expression of these factors is specific to local brain areas(Horvath et al., 1992)(Horvath et al., 1992)(Horvath et al., 1992)(Horvath et al., 1992)(Horvath et al., 1992)(Horvath et al., 1992)(Horvath et al., 1992). In both birds and mammals expression of AgRP is highly localised to the ARC (Phillips-Singh et al., 2003, Ollmann et al., 1997). Expression of NPY is more widespread, being found in the nucleus pretectalis pars ventralis of the telencephalon and within the MBH including the ARC (Wang et al., 2001, Kuenzel and McMurtry, 1988). POMC expression surrounds the 3V, including the ARC and median eminence (Gerets et al.,

2000). Our results are consistent with these observations, indicating the conserved anatomical expression of these feeding related peptides in an arctic galliforme.

The AgRP expression was increased in the LL group compared to the DDc group (**Figure 22B**). The inverse correlation between BM and AgRP expression support the possibility that the expression of AgRP within the MBH are dependent on the BM of the bird (**Figure 24B**). The increase of AgRP may indicate that the bird is in a negative energy balance. These findings are consistent with the association of AgRP gene expression with both acute and chronic food restriction documented in the basal hypothalamus of broiler chickens (Dunn 2013). Within this context it is worth noting the expression of AgRP increased in both the NP12:12 and NP groups which both show reduced mean body mass (**Figure 22B**). Collectively these data suggest that AgRP expression is regulated by energy homeostasis rather than a photoperiodic mechanism. These data are supported by previous work in mammals which document a seasonal body mass is achieved even when AgRP is overexpressed (Jethwa et al., 2010b). Together this may indicate that AgRP is not involved in the regulatory system for a seasonal body weight.

The increase of Dio2 expression correlates with an increased expression of NPY (**Figure 22**, **24A** and Feil! Ugyldig selvreferanse for bokmerke.). Furthermore, NPY expression is independent of body mass indicating a seasonal upregulation of NPY with Dio2 (**Figure 24**). Although the relative expression of Dio2 and NPY have not previously been investigated in birds, experiments in chicken have shown that central injection of T3 is unable to induce NPY (Byerly et al., 2009). As T3 is the metabolic product of the Dio2 enzyme these data bring into question the functional relationship between these two factors. Further study of this correlation will be necessary to define the nature of this association in the Sv. Rock ptarmigan.

The unchanged gene expression of POMC between the experimental groups (**Figure 22D**) indicate that the change in the orexigenic drive on the second order MC4R neuron is caused by an increased biosynthesis of NPY/AgRP rather than a decreased synthesis of POMC. These results are consistent with fasting experiments in chicken (Dunn et al., 2013) and Japanese quail (Phillips-Singh et al., 2003). However, cell-type specific stimulation of POMC neurons for 24 hr decreased food intake in rats suggesting that the role of POMC derived peptides may be different between avians and mammals (Aponte et al., 2011).

Table 7 Photoperiodic effect on physiology and behaviour. Arrows indicate the change of: body mass (BM), voluntary food intake (VFI), activity, and optical density measurements (OD) of Dio2, AgRP and NPY in the mediobasal hypothalamus relative to the DD control group.

PPc group	BM	VFI	Activity	Dio2	AgRP	NPY
DD	↑	↑	-	↑	-	↑
LL	↓↓	↑↑	↑	↑↑↑	↑↑	↑
NP	↓↓	-	↑↑	↑	↑	↑

In previous work on avian feeding neuropeptides (Dunn et al., 2013), found a consistent inverse relationship between BM and AgRP. NPY expression in acute and chronically fasted broiler chickens. Our results do show the same pattern in AgRP expression. Contrastingly the pattern between AgRP and NPY expression differ between our results and the findings of Dunn et al. It is possible that this difference is due to the fine anatomical precision with which our method allowed us to discriminate between the different regions within the MBH. The methods presented here allowed for an area specific measurement of AgRP and NPY in contrast to the Dunn et al. in which whole basal hypothalamic region was measured. NPY is known to be expressed within the MBH in contrast to AgRP which are only expressed within ARC. It is also possible that the feeding mechanisms are not conserved between the chicken and the Sv. rock ptarmigan.

4.4 How is the seasonal change of BM achieved in the Sv. rock ptarmigan?

The data here shows that there is an internal seasonal timing mechanism in the Sv. Rock ptarmigan. The increase in PP cause an increase in activity and metabolic rate which together contribute towards the decrease in BM. The negative change in BM leads to an increase in AgRP expression within the ARC. The increase in Dio2 is also associated with lengthening photoperiods coincides with an increase in NPY. Since there is no correlation between Dio2, AgRP or NPY with VFI it appears that another unmeasured mechanism regulating feeding behaviour is involved. The data presented here can be united through the addition of a photosensitive feeding regulatory mechanism (FRM), which is absent in DD but limits feeding behaviour when activated by long photoperiods. In the NP group the increased orexigenic drive (induced by increased AgRP and NPY expression) is limited through this FRM (**Figure 25**). Contrastingly the FRM is absent in the DD group, which allows the bird to respond to the increased orexigenic drive by increasing VFI. In the LL group the FRM has become photorefractory to long photoperiod and has spontaneously inactivated. The photorefractory reduction in the FRM permits the heightened AgRP/NPY levels within the ARC to drive orexigenic feeding behaviour. The photoperiodic regulation of the FRM ensures that the VFI increase at an appropriate time of year. When the VFI increase the Sv. rock ptarmigan reallocate the increased ingested energy to processes such as moult and reproduction. Therefore, an increase in BM is not observed and the phenotypic summer BM is achieved. The pathways which through the unknown feeding regulatory mechanism is controlled and how VFI is limited remain to be elucidated.

In agreement with previous studies our data suggests that there is a seasonal rheostatic mechanism influencing energy homeostasis (Jethwa et al., 2010a). There are several possible ways the orexigenic signal from AgRP/NPY could be altered through a FRM. Our measurements here represent mRNA, which is known to have a highly tissue and gene specific correlation with peptide abundance (Edfors et al., 2016). Further there are several ways that translation, processing and transport of the peptide could be changed and thus influence the signal strength for the further downstream pathways (Vogel and Marcotte, 2012). For example in mammals AgRP must be cleaved into an active form by prohormone convertases which show seasonal regulation in their activity. The influence of these factors may be critical to the downstream influence of this neuropeptide. Furthermore, the abundance and sensitivity of the cognate receptors (AgRP, MC3/4R; NPY, Y1/Y5 receptors) could vary and influence the transmission of the signal to anorexigenic or second order neurons. It is also possible that seasonal control of feeding behaviour is controlled by higher order pathways. In the Arctic charr (Salvelinus alpinus), a highly seasonal fish species, the annual feeding cycle is not reflected in central appetite regulators (Striberny et al., 2015). Studies in mammals reveal that male Siberian hamsters display a seasonality in body weight, food intake, pelage and reproduction despite monosodium glutamate-

induced lesions of the arcuate nucleus (Ebling et al., 1998). This may indicate that the regulatory system for a seasonal body weight in the Sv. rock ptarmigan resides outside the ARC. Additionally the increase of AgRP but no increase in VFI may be explained by a stronger drive for territorial behaviour. This territoriality would supress the feeding, even when an orexigenic signal is present.

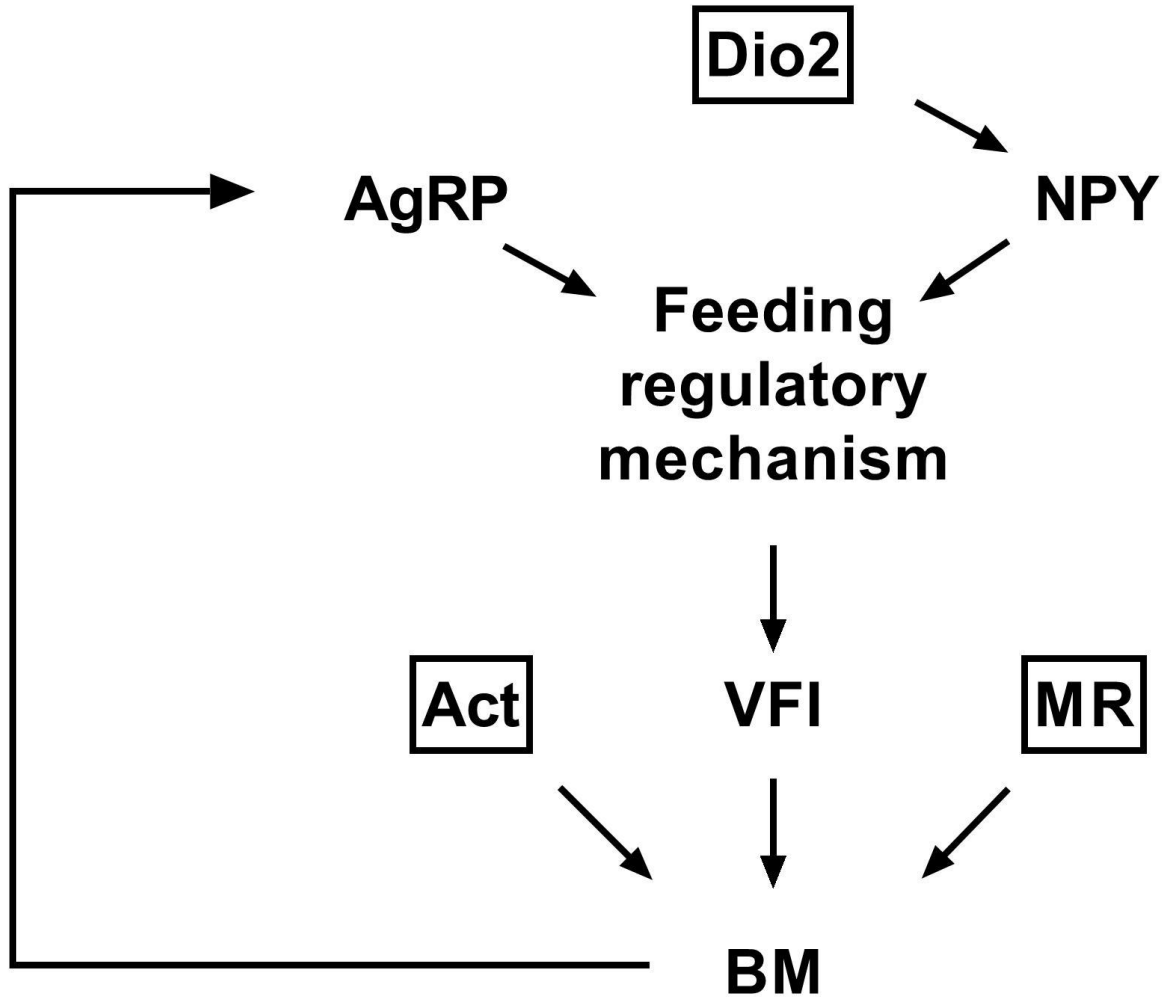

Figure 25 Schematic of the photoperiodic influence on body mass in a Sv. rock ptarmigan. Boxes are factors known to be influenced by PP. The remaining are factors linked to these photoperiodic responses. As here shown Dio2 correlates with NPY expression. The upregulation of NPY is through photoperiodic sensitive unknown feeding regulatory mechanisms tempered and thus the increased orexigenic signal is not reflected in increased VFI. As PP increase, activity increase and correlate with a decrease in BM. The negative change in BM is mirrored in increased AgRP expression. Both increased AgRP and NPY expression is not reflected in VFI until the feeding regulatory mechanisms are released through photorefractoriness. Then the increased AgRP/NPY signal is associated with an increase in VFI. In this way, light sensitive feeding regulatory mechanisms seems to in a seasonal way limit food intake to reach a seasonal appropriate BM. Abbreviations: Dio2- type 2 deiodinase, AgRP- Agouti related peptide, NPY- neuropeptide Y, Act – activity, VFI- voluntary food intake, MR – metabolic rate and BM – body mass.

Outlook

The present study has focused on correlating changes in physiology and behaviour with the expression of a small number of well characterised genes in the MBH. The inclusion of several other feeding related factors would improve our understanding of the involvement of ARC in a seasonal body weight set-point in the brain. Amongst these, characterisation of the anorexigenic peptide cocaine- and amphetamine-regulated transcript (CART) would be a particularly clear target. CART is expressed in POMC neurons and intracerebroventricular injections of the peptide have been shown to reduce feeding in rodents (Stanley et al., 2001, Lambert et al., 1998).

Through this experiment, samples of skin, liver, ceca, intestine, fat, and blood were collected for future investigation of the photoperiodic effect on the connection between the periphery and the brain. These samples will be invaluable for the further characterisation of the birds in this experiment. This material should be used to test for photoperiodic influence on circulating hormones such as ghrelin, insulin and CCK.

To better understand the seasonal change in energy expenditure, further characterisation of the impact of photoperiod on metabolic rate through indirect calorimetry would be of great interest. In addition, the influence of the large seasonal variation in relative fat mass on energy homeostasis in the Sv. rock ptarmigan could be investigated through glucose and insulin tolerance tests.

Future research should focus on how a hypothesised feeding regulatory mechanism is involved in the seasonal body weight set-point in the Sv. rock ptarmigan. This could be achieved through identification of neuron populations in the MBH with the use of co-localization studies. Previous work has shown that tanycytes perform an essential role as nutrient sensors, display a seasonal gene expression and connect with DMH, PVH and ARC which are regions within the MBH highly involved in energy homeostasis. Collectively, tanycytes may be an integration point for a seasonal body weight set-point. Exploring the possibility of a functional link between tanycytes and the seasonal rheostatic mechanism influencing energy homeostasis should be a clear aim of future research.

5 Conclusion

This study is the first to investigate photoperiodic control of central appetite regulation genes in Svalbard rock ptarmigan. Captive birds were exposed to three different photoperiodic treatments and sampled at 6 different timepoints. POMC was unaffected by photoperiodic treatment, however expression of feeding related peptides was strongly influenced by the experiments. The expression of AgRP was induced in the groups with negative change in body weight. Similar to previous work in seasonal models the high expression of AgRP was not associated with elevated VFI but was instead reflective of seasonal status. The expression of NPY correlated with the expression of the Dio2 which itself is regulated by long PPs but also an SP refractory mechanism. Similar to AgRP, NPY expression does not correlate with feeding behaviour. Collectively these data suggest that additional feeding related mechanisms which are sensitive to PP, but also display a refractoriness to long PPs temper the influence of AgRP/NPY neurons in the MBH.

Works cited

ANDERMANN, M. L. & LOWELL, B. B. 2017. Toward a Wiring Diagram Understanding of Appetite Control. *Neuron,* 95**,** 757-778.

APONTE, Y., ATASOY, D. & STERNSON, S. M. 2011. AGRP neurons are sufficient to orchestrate feeding behavior rapidly and without training. *Nature Neuroscience,* 14**,** 351.

APPENROTH, D. 2016. Core body temperature cycles in captive Svalbard rock ptarmigan (Lagopus muta hyperborea). The arctic university of Norway.

APPENROTH, D. 2017. Thyrotrophin expression in the pars tuberalis in Svalbard rock ptarmigan.

BALSALOBRE, A., BROWN, S. A., MARCACCI, L., TRONCHE, F., KELLENDONK, C., REICHARDT, H. M., SCHÜTZ, G. & SCHIBLER, U. 2000. Resetting of Circadian Time in Peripheral Tissues by Glucocorticoid Signaling. *Science,* 289**,** 2344-2347.

BARTNESS, T. J., POWERS, J. B., HASTINGS, M. H., BITTMAN, E. L. & GOLDMAN, B. D. 1993. The timed infusion paradigm for melatonin delivery: what has it taught us about the melatonin signal, its reception, and the photoperiodic control of seasonal responses? *J Pineal Res,* 15**,** 161-90.

BINKLEY, S. & MOSHER, K. 1985. Oral melatonin produces arrhythmia in sparrows. *Experientia,* 41**,** 1615-1617.

BLIX, A. S. 2016. Adaptations to polar life in mammals and birds. *The Journal of Experimental Biology,* 219**,** 1093-1105.

BOLBOREA, M. & DALE, N. 2013. Hypothalamic tanycytes: potential roles in the control of feeding and energy balance. *Trends in Neurosciences,* 36**,** 91-100.

BOSWELL, T. & DUNN, I. C. 2017. Regulation of Agouti-Related Protein and Pro-Opiomelanocortin Gene Expression in the Avian Arcuate Nucleus. *Frontiers in Endocrinology,* 8.

BOSWELL, T. & TAKEUCHI, S. 2005. Recent developments in our understanding of the avian melanocortin system: Its involvement in the regulation of pigmentation and energy homeostasis. *Peptides,* 26**,** 1733-1743.

BRANDSTÄTTER, R. 2003. Encoding Time of Day and Time of Year by the Avian Circadian System. *Journal of Neuroendocrinology,* 15**,** 398-404.

BÜNNING, E. 1937. Die endonome Tagesrhythmik als Grundlage der photoperiodischen Reaktion. *Ber. Deut. Bot. Ges.,* 54**,** 590-607.

BYERLY, M. S., SIMON, J., LEBIHAN-DUVAL, E., DUCLOS, M. J., COGBURN, L. A. & PORTER, T. E. 2009. Effects of BDNF, T3, and corticosterone on expression of the hypothalamic obesity gene network in vivo and in vitro. *American Journal of Physiology-Regulatory, Integrative and Comparative Physiology,* 296**,** R1180-R1189.

DENBOW, D. M. & MYERS, R. D. 1982. Eating, drinking and temperature responses to intracerebroventricular cholecystokinin in the chick. *Peptides,* 3**,** 739-43.

DODD, A. N., SALATHIA, N., HALL, A., KÉVEI, E., TÓTH, R., NAGY, F., HIBBERD, J. M., MILLAR, A. J. & WEBB, A. A. R. 2005. Plant Circadian Clocks Increase Photosynthesis, Growth, Survival, and Competitive Advantage. *Science,* 309**,** 630-633.

DUNN, I. C., W., W. P., V., S. T., V., S., B., D. E. R. & T., B. 2013. Hypothalamic Agouti-Related Protein Expression Is Affected by Both Acute and Chronic Experience of Food Restriction and Re-Feeding in Chickens. *Journal of Neuroendocrinology,* 25**,** 920-928.

E. J. FØRLAND (ED), R. E. BENESTAD, F. FLATØY, I. HANSSEN-BAUER, J. E. HAUGEN, K. ISAKSEN, A. SORTEBERG & ÅDLANDSVIK, B. 2009. Climate development in North Norway and the Svalbard region during 1900–2100. Norwegian Polar Institute.

EBLING, F. J., ARTHURS, O. J., TURNEY, B. W. & CRONIN, A. S. 1998. Seasonal neuroendocrine rhythms in the male Siberian hamster persist after monosodium glutamate-induced lesions of the arcuate nucleus in the neonatal period. *J Neuroendocrinol,* 10**,** 701-12.

EDFORS, F., DANIELSSON, F., HALLSTRÖM, B. M., KÄLL, L., LUNDBERG, E., PONTÉN, F., FORSSTRÖM, B. & UHLÉN, M. 2016. Gene‐specific correlation of RNA and protein levels in human cells and tissues. *Molecular Systems Biology,* 12.

FOLLETT, B. K., MATTOCKS, P. W. & FARNER, D. S. 1974. Circadian Function in the Photoperiodic Induction of Gonadotropin Secretion in the White-crowned Sparrow

(*Zonotrichia leucophrys gambelii*). *Proceedings of the National Academy of Sciences,* 71**,** 1666-1669.
FURUSE, M., TACHIBANA, T., OHGUSHI, A., ANDO, R., YOSHIMATSU, T. & DENBOW, D. M. 2001. Intracerebroventricular injection of ghrelin and growth hormone releasing factor inhibits food intake in neonatal chicks. *Neuroscience Letters,* 301**,** 123-126.
GERETS, H. H., PEETERS, K., ARCKENS, L., VANDESANDE, F. & BERGHMAN, L. R. 2000. Sequence and distribution of pro-opiomelanocortin in the pituitary and the brain of the chicken (Gallus gallus). *J Comp Neurol,* 417**,** 250-62.
HEIGL, S. & GWINNER, E. 1995. Synchronization of Circadian Rhythms of House Sparrows by Oral Melatonin: Effects of Changing Period. *Journal of Biological Rhythms,* 10**,** 225-233.
HONDA, K., KAMISOYAMA, H., SANEYASU, T., SUGAHARA, K. & HASEGAWA, S. 2007. Central administration of insulin suppresses food intake in chicks. *Neuroscience Letters,* 423**,** 153-157.
HORVATH, T. L., NAFTOLIN, F., KALRA, S. P. & LERANTH, C. 1992. Neuropeptide-Y innervation of beta-endorphin-containing cells in the rat mediobasal hypothalamus: a light and electron microscopic double immunostaining analysis. *Endocrinology,* 131**,** 2461-2467.
IMS, R. A. A., INGER G.; FUGLEI, EVA; PEDERSEN, ÅSHILD Ø.; YOCCOZ, NIGEL G. 2014. An assessment of MOSJ: the state of the terrestrial environment in Svalbard. Norwegian Polar Institute
IPPC 2014. Climate Change 2014: Synthesis Report. Contribution of Working Groups I, II and III to the Fifth Assessment Report of the Intergovernmental Panel on Climate Change. R.K. Pachauri and L.A. Meyer ed. Geneva, Switzerland.
JETHWA, P. H., WARNER, A., FOWLER, M. J., MURPHY, M., BACKER, M. W. D., ADAN, R. A. H., BARRETT, P., BRAMELD, J. M. & EBLING, F. J. P. 2010a. Short‐Days Induce Weight Loss in Siberian Hamsters Despite Overexpression of the Agouti‐Related Peptide Gene. *Journal of Neuroendocrinology,* 22**,** 564-575.
JETHWA, P. H., WARNER, A., FOWLER, M. J., MURPHY, M., DE BACKER, M. W., ADAN, R. A., BARRETT, P., BRAMELD, J. M. & EBLING, F. J. 2010b. Short-days induce weight loss in Siberian hamsters despite overexpression of the agouti-related peptide gene. *J Neuroendocrinol,* 22**,** 564-75.
KUENZEL, W. J. & MCMURTRY, J. 1988. Neuropeptide Y: Brain localization and central effects on plasma insulin levels in chicks. *Physiology & Behavior,* 44**,** 669-678.
LAMBERT, P. D., COUCEYRO, P. R., MCGIRR, K. M., DALL VECHIA, S. E., SMITH, Y. & KUHAR, M. J. 1998. CART peptides in the central control of feeding and interactions with neuropeptide Y. *Synapse,* 29**,** 293-8.
LINDGÅRD, K., STOKKAN, K.-A. & NÄSLUND, S. 1995. Annual changes in body mass in captive Svalbard ptarmigan: role of changes in locomotor activity and food intake. *Journal of Comparative Physiology B,* 165**,** 445-449.
MARCELO, O. D. & HORVATH, T. L. 2010. *Neural regulation of food intake and energy balance* [Online]. Nature reviews neuroscience: Nature publisher group. [Accessed 15.01.18 2018].
MARCELO, O. D. & HORVATH, T. L. 2012. Limitations in anti-obesity drug development: the critical role of hunger-promoting neurons. *Nature Reviews Drug Discovery,* 11**,** 675-691.
MIERA, C. S. D., HANON, E. A., DARDENTE, H., BIRNIE, M., SIMONNEAUX, V., LINCOLN, G. A. & HAZLERIGG, D. G. 2013. Circannual Variation in Thyroid Hormone Deiodinases in a Short‐Day Breeder. *Journal of Neuroendocrinology,* 25**,** 412-421.
MORTENSEN, A. & BLIX, A. S. 1985. Seasonal Changes in the Effects of Starvation on Metabolic Rate and Regulation of Body Weight in Svalbard Ptarmigan. *Ornis Scandinavica (Scandinavian Journal of Ornithology),* 16**,** 20-24.
MORTENSEN, A. & BLIX, A. S. 1986. Seasonal Changes in Resting Metabolic Rate and Mass-Specific Conductance in Svalbard Ptarmigan, Norwegian Rock Ptarmigan and Norwegian Willow Ptarmigan. *Ornis Scandinavica (Scandinavian Journal of Ornithology),* 17**,** 8-13.
MORTENSEN, A., UNANDER, S., KOLSTAD, M. & BLIX, A. S. 1983. Seasonal Changes in Body Composition and Crop Content of Spitzbergen Ptarmigan Lagopus mutus hyperboreus. *Ornis Scandinavica (Scandinavian Journal of Ornithology),* 14**,** 144-148.

MORTON, G. J., CUMMINGS, D. E., BASKIN, D. G., BARSH, G. S. & SCHWARTZ, M. W. 2006. Central nervous system control of food intake and body weight. *Nature,* 443**,** 289.

MROSOVSKY, N. & FISHER, K. C. 1970. Sliding set points for body weight in ground squirrels during the hibernation season. *Canadian Journal of Zoology,* 48**,** 241-247.

MURPHY, M. & EBLING, F. J. P. 2011. The Role of Hypothalamic Tri-Iodothyronine Availability in Seasonal Regulation of Energy Balance and Body Weight. *Journal of Thyroid Research,* 2011**,** 7.

NAKANE, Y., IKEGAMI, K., ONO, H., YAMAMOTO, N., YOSHIDA, S., HIRUNAGI, K., EBIHARA, S., KUBO, Y. & YOSHIMURA, T. 2010. A mammalian neural tissue opsin (Opsin 5) is a deep brain photoreceptor in birds. *Proceedings of the National Academy of Sciences of the United States of America,* 107**,** 15264-15268.

NAKANE, Y. & YOSHIMURA, T. 2014. Universality and diversity in the signal transduction pathway that regulates seasonal reproduction in vertebrates. *Frontiers in Neuroscience,* 8.

NAKAO, N., ONO, H., YAMAMURA, T., ANRAKU, T., TAKAGI, T., HIGASHI, K., YASUO, S., KATOU, Y., KAGEYAMA, S., UNO, Y., KASUKAWA, T., IIGO, M., SHARP, P. J., IWASAWA, A., SUZUKI, Y., SUGANO, S., NIIMI, T., MIZUTANI, M., NAMIKAWA, T., EBIHARA, S., UEDA, H. R. & YOSHIMURA, T. 2008. Thyrotrophin in the pars tuberalis triggers photoperiodic response. *Nature,* 452**,** 317.

NANDA, K. K. & HAMNER, K. C. 1958. Studies on the Nature of the Endogenous Rhythm Affecting Photoperiodic Response of Biloxi Soybean. *Botanical Gazette,* 120**,** 14-25.

OLLMANN, M. M., WILSON, B. D., YANG, Y.-K., KERNS, J. A., CHEN, Y., GANTZ, I. & BARSH, G. S. 1997. Antagonism of Central Melanocortin Receptors in Vitro and in Vivo by Agouti-Related Protein. *Science,* 278**,** 135-138.

PANDA, S., ANTOCH, M. P., MILLER, B. H., SU, A. I., SCHOOK, A. B., STRAUME, M., SCHULTZ, P. G., KAY, S. A., TAKAHASHI, J. S. & HOGENESCH, J. B. 2002. Coordinated Transcription of Key Pathways in the Mouse by the Circadian Clock. *Cell,* 109**,** 307-320.

PARTCH, C. L., GREEN, C. B. & TAKAHASHI, J. S. 2014. Molecular architecture of the mammalian circadian clock. *Trends in Cell Biology,* 24**,** 90-99.

PHILLIPS-SINGH, D., LI, Q., TAKEUCHI, S., OHKUBO, T., SHARP, P. J. & BOSWELL, T. 2003. Fasting differentially regulates expression of agouti-related peptide, pro-opiomelanocortin, prepro-orexin, and vasoactive intestinal polypeptide mRNAs in the hypothalamus of Japanese quail. *Cell and Tissue Research,* 313**,** 217-225.

PITTENDRIGH, C. S. 1972. Circadian Surfaces and the Diversity of Possible Roles of Circadian Organization in Photoperiodic Induction. *Proceedings of the National Academy of Sciences,* 69**,** 2734-2737.

SCHWARTZ, M. W., WOODS, S. C., PORTE, D., JR., SEELEY, R. J. & BASKIN, D. G. 2000. Central nervous system control of food intake. *Nature,* 404**,** 661-71.

SEROUSSI, E., CINNAMON, Y., YOSEFI, S., GENIN, O., SMITH, J. G., RAFATI, N., BORNELÖV, S., ANDERSSON, L. & FRIEDMAN-EINAT, M. 2016. Identification of the Long-Sought Leptin in Chicken and Duck: Expression Pattern of the Highly GC-Rich Avian leptin Fits an Autocrine/Paracrine Rather Than Endocrine Function. *Endocrinology,* 157**,** 737-751.

SILVERIN, B., WINGFIELD, J., STOKKAN, K.-A., MASSA, R., JÄRVINEN, A., ANDERSSON, N.-Å., LAMBRECHTS, M., SORACE, A. & BLOMQVIST, D. 2008. Ambient temperature effects on photo induced gonadal cycles and hormonal secretion patterns in Great Tits from three different breeding latitudes. *Hormones and Behavior,* 54**,** 60-68.

SONG, Z., LIU, L., YUE, Y., JIAO, H., LIN, H., SHEIKHAHMADI, A., EVERAERT, N., DECUYPERE, E. & BUYSE, J. 2012. Fasting alters protein expression of AMP-activated protein kinase in the hypothalamus of broiler chicks (Gallus gallus domesticus). *General and Comparative Endocrinology,* 178**,** 546-555.

STANLEY, S. A., SMALL, C. J., MURPHY, K. G., RAYES, E., ABBOTT, C. R., SEAL, L. J., MORGAN, D. G., SUNTER, D., DAKIN, C. L., KIM, M. S., HUNTER, R., KUHAR, M., GHATEI, M. A. & BLOOM, S. R. 2001. Actions of cocaine- and amphetamine-regulated

transcript (CART) peptide on regulation of appetite and hypothalamo-pituitary axes in vitro and in vivo in male rats. *Brain Res,* 893**,** 186-94.
STEINLECHNER, S., HELDMAIER, G. & BECKER, H. 1983. The seasonal cycle of body weight in the Djungarian hamster: photoperiodic control and the influence of starvation and melatonin. *Oecologia,* 60**,** 401-405.
STOKKAN, K.-A. 1992. Energetics and Adaptations to Cold in Ptarmigan in Winter. *Ornis Scandinavica (Scandinavian Journal of Ornithology),* 23**,** 366-370.
STOKKAN, K.-A., HARVEY, S., KLANDORF, H., UNANDER, S. & BLIX, A. S. 1985. Endocrine changes associated with fat deposition and mobilization in Svalbard ptarmigan (Lagopus mutus hyperboreus). *General and Comparative Endocrinology,* 58**,** 76-80.
STOKKAN, K.-A., SHARP, P. J. & MOSS, R. 1982. Development of photorefractoriness in willow ptarmigan (Lagopus lagopus lagopus) and red grouse (Lagopus lagopus scoticus) exposed to different photoperiods. *General and Comparative Endocrinology,* 46**,** 281-287.
STOKKAN, K.-A., SHARP, P. J. & UNANDER, S. 1986. The annual breeding cycle of the high-arctic svalbard ptarmigan (Lagopus mutus hyperboreus). *General and Comparative Endocrinology,* 61**,** 446-451.
STRIBERNY, A., RAVURI, C. S., JOBLING, M. & JORGENSEN, E. H. 2015. Seasonal Differences in Relative Gene Expression of Putative Central Appetite Regulators in Arctic Charr (Salvelinus alpinus) Do Not Reflect Its Annual Feeding Cycle. *PLoS One,* 10**,** e0138857.
UNANDER, S. & STEEN, J. B. 1985. Behaviour and Social Structure in Svalbard Rock Ptarmigan Lagopus mutus hyperboreus. *Ornis Scandinavica (Scandinavian Journal of Ornithology),* 16**,** 198-204.
VOGEL, C. & MARCOTTE, E. M. 2012. Insights into the regulation of protein abundance from proteomic and transcriptomic analyses. *Nat Rev Genet,* 13**,** 227-32.
VON GALL, C., DUFFIELD, G. E., HASTINGS, M. H., KOPP, M. D. A., DEHGHANI, F., KORF, H.-W. & STEHLE, J. H. 1998. CREB in the Mouse SCN: A Molecular Interface Coding the Phase-Adjusting Stimuli Light, Glutamate, PACAP, and Melatonin for Clockwork Access. *The Journal of Neuroscience,* 18**,** 10389-10397.
WAGNER, G. C., JOHNSTON, J. D., CLARKE, I. J., LINCOLN, G. A. & HAZLERIGG, D. G. 2008. Redefining the Limits of Day Length Responsiveness in a Seasonal Mammal. *Endocrinology,* 149**,** 32-39.
WANG, X., DAY, J. R. & VASILATOS-YOUNKEN, R. 2001. The distribution of neuropeptide Y gene expression in the chicken brain. *Molecular and Cellular Endocrinology,* 174**,** 129-136.
WOELFLE, M. A., OUYANG, Y., PHANVIJHITSIRI, K. & JOHNSON, C. H. 2004. The Adaptive Value of Circadian Clocks: An Experimental Assessment in Cyanobacteria. *Current Biology,* 14**,** 1481-1486.
YOSHIMURA, T., YASUO, S., WATANABE, M., IIGO, M., YAMAMURA, T., HIRUNAGI, K. & EBIHARA, S. 2003. Light-induced hormone conversion of T4 to T3 regulates photoperiodic response of gonads in birds. *Nature,* 426**,** 178.
YUAN, J., GILBERT, E. R. & CLINE, M. A. 2017. The central anorexigenic mechanism of amylin in Japanese quail (Coturnix japonica) involves pro-opiomelanocortin, calcitonin receptor, and the arcuate nucleus of the hypothalamus. *Comparative Biochemistry and Physiology Part A: Molecular & Integrative Physiology,* 210**,** 28-34.

6 Appendix

6.1 Measurements from each sampling point

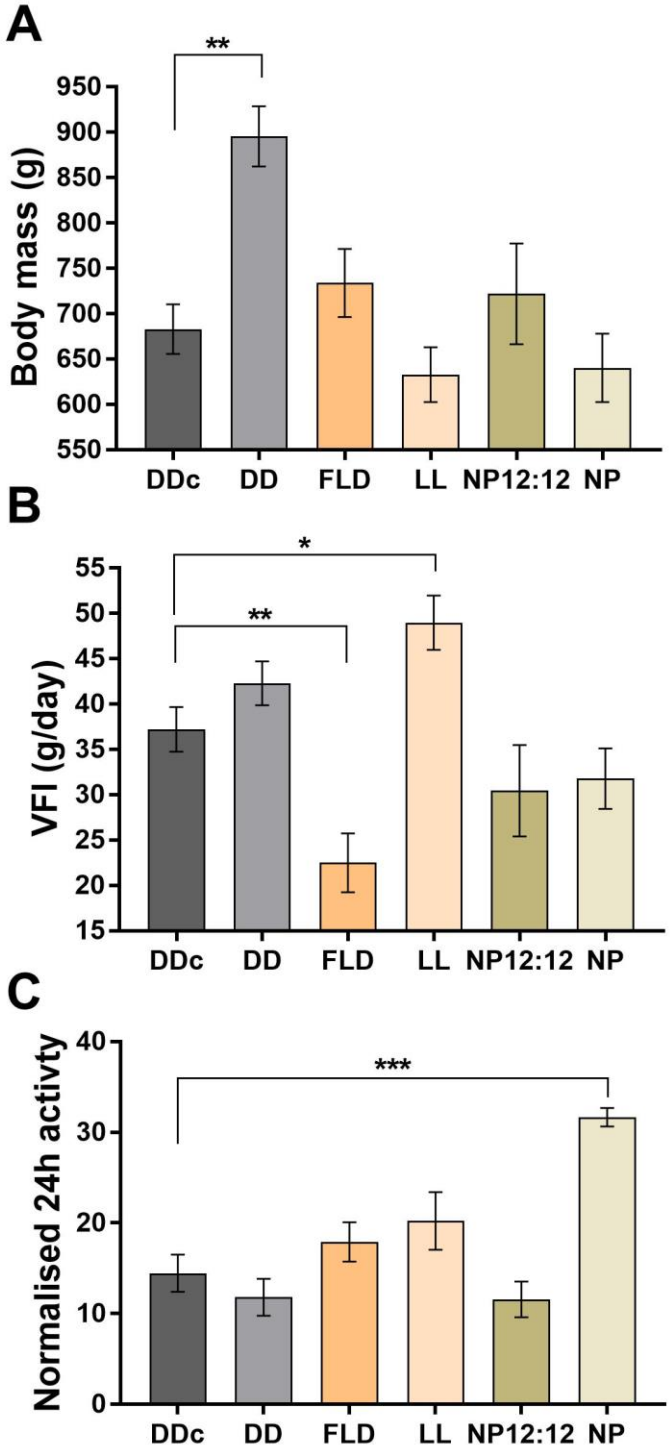

Figure 26 Background information for each sampling point. (A) Body mass in grams for each bird at each sampling point (n=4-6). (B) Mean voluntary food intake (VFI) for representative animals within each PP group in 6-10 days prior to each timepoint (n=3-5). (C) Mean normalised 24hour activity for representative animals within each PP group in 4 days prior to each timepoint (n=4-6). *P<0.05, **P<0.01, ****P<0.0001. 1way ANOVA post-hoc Dunnett`s multiple comparisons test was used to detect differences between the DDcontrol (DDc) and the remaining groups. Constant darkness (DD), first long day (FLD), constant light (LL), natural photoperiod 12:12 (NP12:12), natural photoperiod (NP).

6.2 NPY expression outside region of interest

In all groups a high expression of NPY in a localized area was detected in the cross-section (**Figure 27**B).

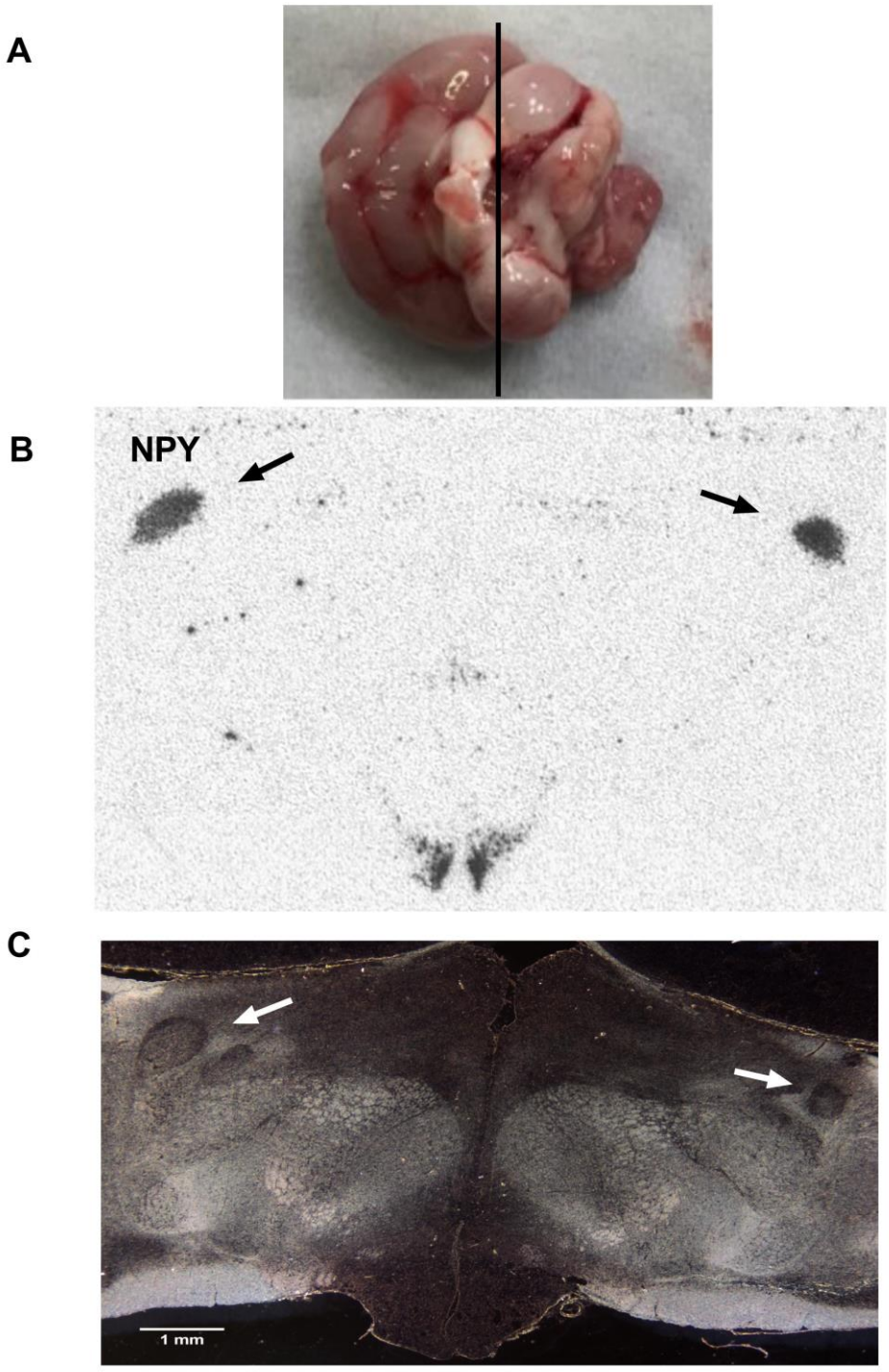

Figure 27 NPY expression. (A) Captive Svalbard rock ptarmigan brain ventral side facing up, line indicate the region where the cross-section in B was performed (photo: Fredrik Markussen). (B) Autoradiograph of NPY expression. Arrow indicate area of high expression found in all birds. (C) The respective slide showed in B, toloudine stained and imaged through a microscope. White arrows indicate the nuclei that correspond to the heavily labelled area of NPY in B.

6.3 The sick bird

In the NP12:12 group, one female was noted to be sick prior to the sampling (**Table 8**). The bird exhibited a decreased appetite and irregular behaviour. The measurement of the mean VFI over 6 days prior to this groups endpoint was only 6.3 grams, and the BM was 570 grams. Both measurements deviated from the rest of the group. The OD measurements of AgRP in this bird was 8.5 times higher than the others (>2SD). The alignment of the observed behaviour, BM, VFI and AgRP expression for this individual strengthens the relationship found between BM and AgRP for the whole group. In addition, it demonstrates the applicability of the use of ISH as a method to correlate physiological measurements with changes in central gene expression within the MBH.

Table 8 An outlier was a sick bird. One female in the NP12:12 group deviated from the rest of the group in terms of, BM (grams), mean VFI (grams/day) and optical density (OD) measurements of AgRP.

PP-group	BM (g)	Mean VFI (g/day)	AgRP (OD)
NP12:12	570	6.3	0.480

6.4 Antisense and sense; the probes specificity

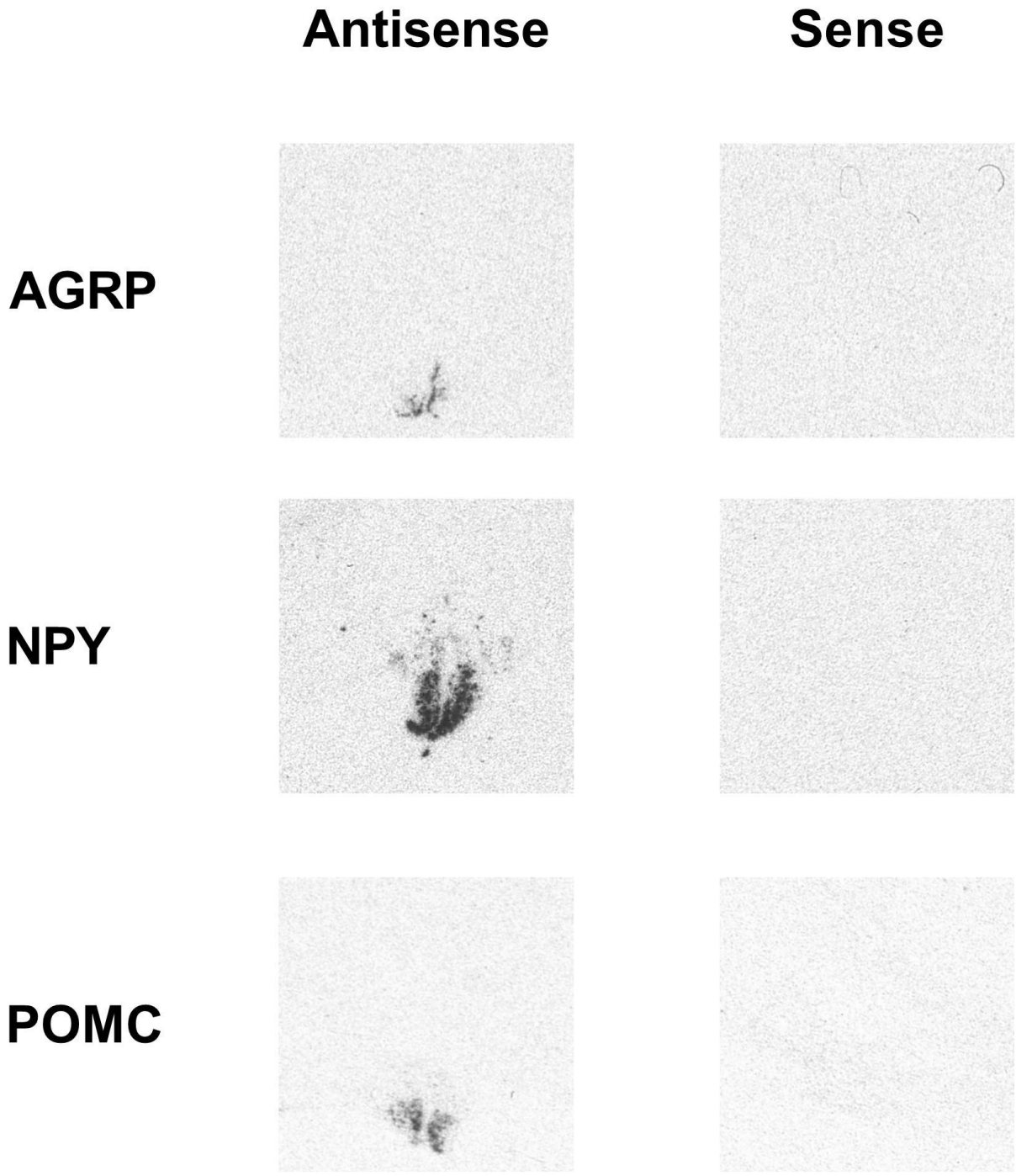

Figure 28 radioactive autoradiographs of antisense and sense. On a test brain the riboprobe synthesized from cloned cDNA for the appetite genes AgRP, NPY and POMC were tested to determine the specific binding. In the same ISH a sense was applied to demonstrate that no signal was detected if no specific binding occurred. Together this show that the probe used (antisense) has a specific binding to the mRNA of interest in the expected region.

6.5 Actograms

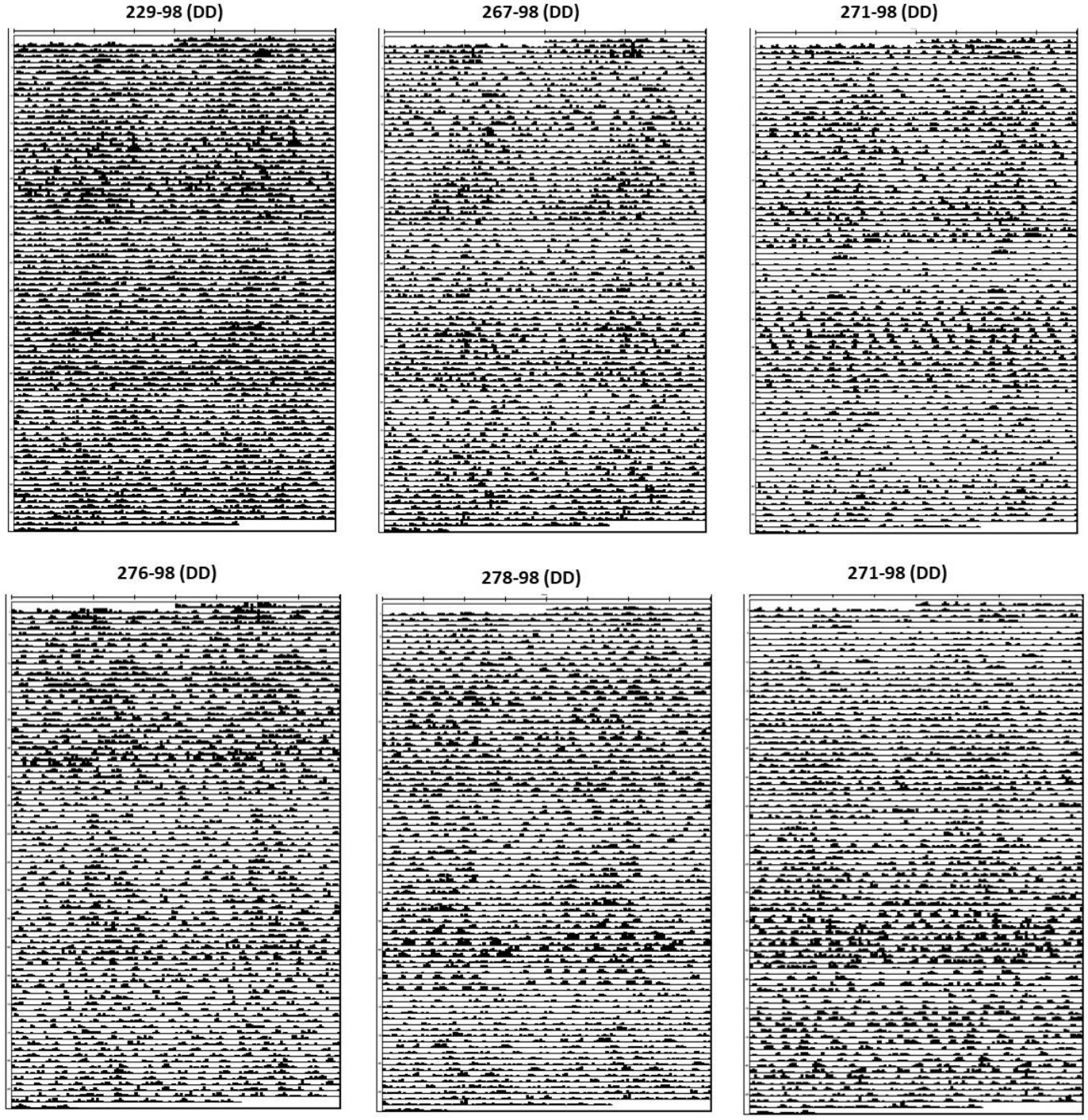

Figure 29 Double plotted actograms for Sv. Rock ptarmigan in DD. Activity is in 20 minutes bins divided by the 99 percentiles and the upper and lower limits ranging from 0 (no activity) and 1 (99 percentiles). The X-axis depicts clock hours and the y-axis are experimental weeks. Each line on the actogram represent 2 days with the second day being repeated in the next line.

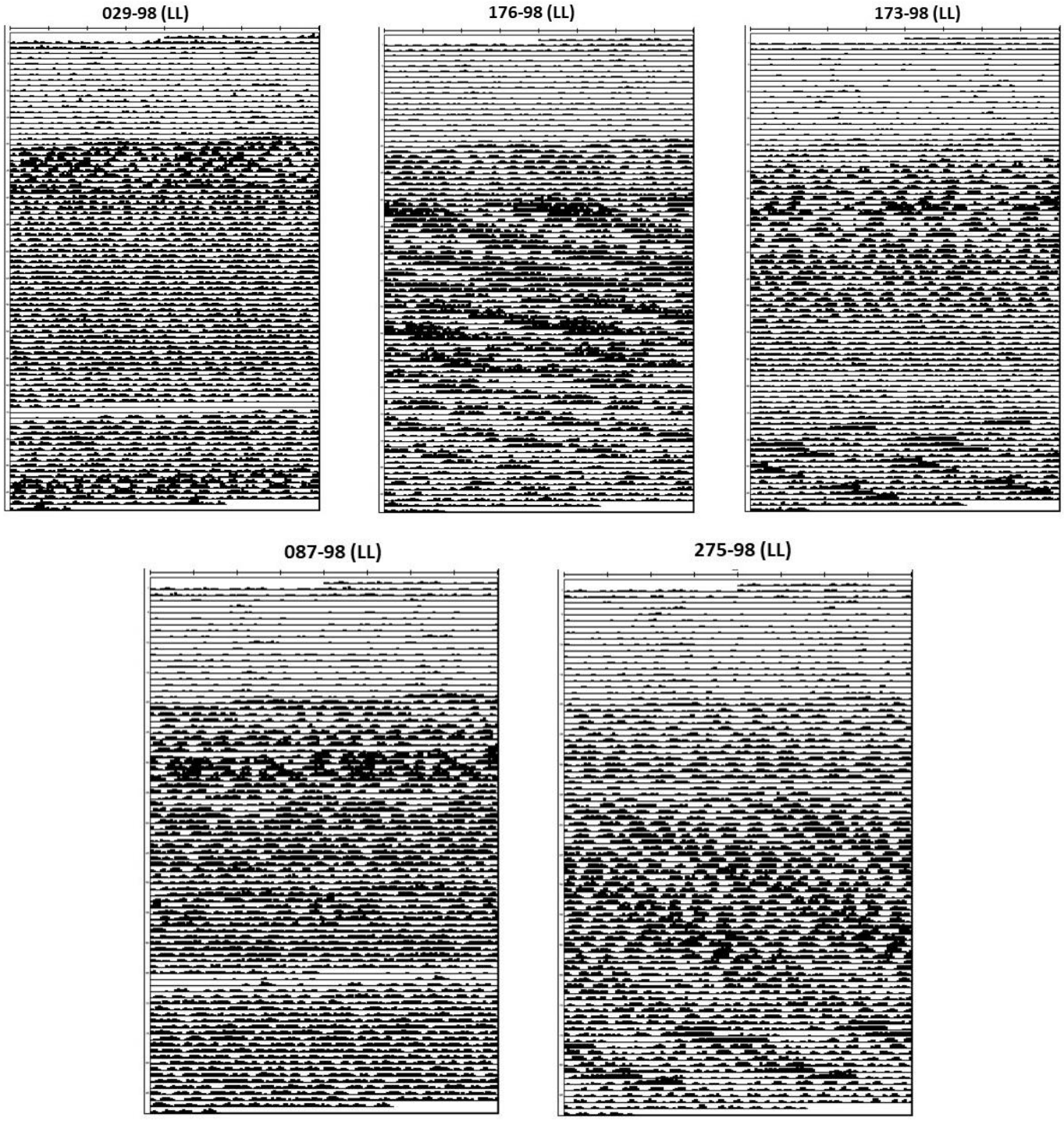

Figure 30 Double plotted actograms of Sv. Rock ptarmigan in LL. Activity is in 20 minutes bins divided by the 99 percentiles and the upper and lower limits ranging from 0 (no activity) and 1 (99 percentiles). The X-axis depicts clock hours and the y-axis are experimental weeks. Each line on the actogram represent 2 days with the second day being repeated in the next line. For bird 066-98 no measurements were obtained until experimental start. To allow comparison with the other birds, this period is filled with 0 activity.

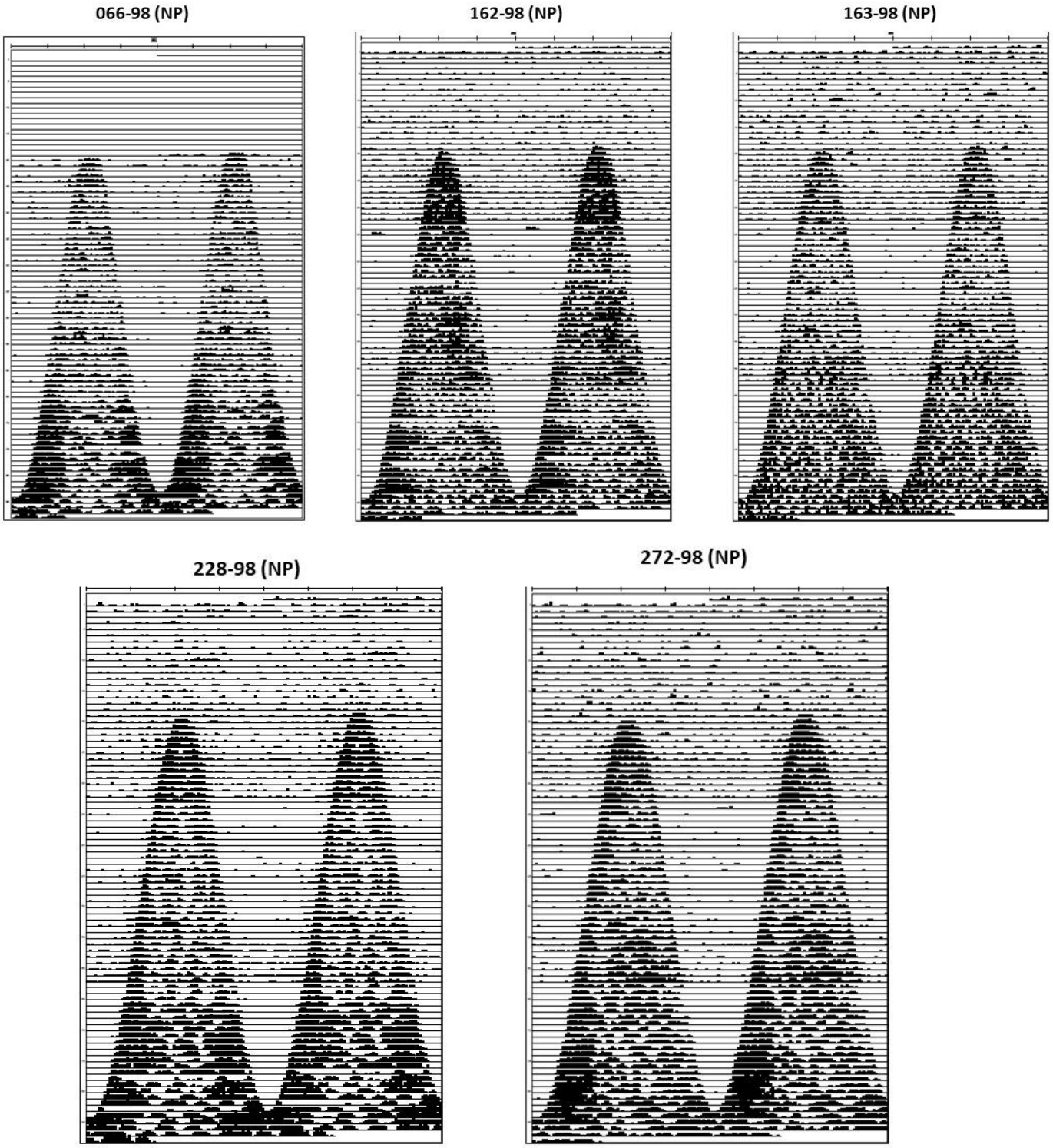

Figure 31 Double plotted actograms for Sv. Rock ptarmigan under NP. Activity is in 20 minutes bins divided by the 99 percentiles and the upper and lower limits ranging from 0 (no activity) and 1 (99 percentiles). The X-axis depicts clock hours and the y-axis are experimental weeks. Each line on the actogram represent 2 days with the second day being repeated in the next line. For bird 066-98 no measurements were obtained until experimental start. To allow comparison with the other birds, this period was filled with 0 activity.

6.6 Sequences

Clones AgRP (461 bp)

ACCATGCTGAACGCGCTGCTGCTGTGCTACGGGCTGCTGCAGGGGATCCAGGCCATCCTC
AGCTCGGAGCTCAGCCACAGCCCCCTGCAGAAGATGAGCTCTGGGCTGGAGGAGGCAGA
CAGAGCCCGCTACCCCAGCCTGCTGCACAAGGCCAAGGAGCTGCCAGTGGAGCTTGCTG
GAGCTATTCCCAGGCCGGACTCGGATCAGATGGAGGTGCATGAAGGTGATGGTAACCTC
CTGCAGAAAAGCAGCGTGCTGGAACCACAGGCATTGTCCACGGCCCTGCAAGCTGCAGG
CAGGGAGGAGCGGAGCTCCCCTCGCCGTTGTGTCCGTCTCCTGGAGTCCTGCCTGGGCCA
CCAGATCCCCTGCTGCGACCCCTGTGCCACCTGCTACTGCCGGTTTTTCAACGCCTTCTGC
TACTGCAGGAAGATCAGCACCACCTTCCCATGCGGCAAGAACTA

Clones NPY (370 bp)

CAATGGCTGCATGCACTGGGAATGATGCTATGATTTGCTTCAGAGGAGTGAAGTATGAAT
TGAAAACTAGGAAAAATTTGGATGGTGTGCTGCAAATCCCATCACCACATCGAAGGGTCT
TCAAACCGGGATCTAGGAATGTTTTCTGTGCTTTCCCTCAACAAGAGGTCTGAGATCAGT
GTCTCTGGGCTTGATCTCTTTCCGTACCTCTGCCTGGTGATGAGGTTGATGTAGTGCCTCA
GAGCCGAGTAGTATCTGGCCATGTCCTCTGCGGGAGCGTCCTCGCCGGGGCTGTCCGGTT
TGGAGGGGTACGCTTCTGCCAGCGTCCCCAGGCAGACCAGCAGCGACAGGGCGAAAGTC
AGCACCGACA

Clones POMC (497 bp)

GAACAGAGTCATCAGCGGCGTCTGGCTGTGCTCCAGGGTCATGAAGCCGCCGTAGCGCTT
GTCCTTCAGCGGCGCGTGCCAGCGGAAGTGCCGCATGCGGTACGAGCCGCCGTCCTTCTT
TTCCTCCTCGCCTTCCTCCTCCTGCTCTTCCTCTTCCAAGAGGCCGAGGGGATCCTCGTCG
GCCGCCATCTCCCTCCGGAACTCCATGGGGTAGCTCTCGGCCGACTCCTCGTCCACGCTGT
TGGGGTACACCTTGATGGGTCTCCTCTTCCGTCCCACCGGTTTGCCCCAGCGGAAATGCTC
CATGGAGTAGGAGCGCTTCCCTTCCTCTCGCTCCAACCCTTCTCCATCTTCCTCCTCCCCG
GGGGGGCGGTGGGGTGATGTGATGGGCAGGGCGAGGCCGGCCACCTCCTCCCTTTTATGC
CCTCCGCTGCTGCTGTTGCGACGGCCGAACTTGTTCCAGCGGAAATGGCTCATCACGTAC
TTGCGGATGCTCT

6.7 Room plans

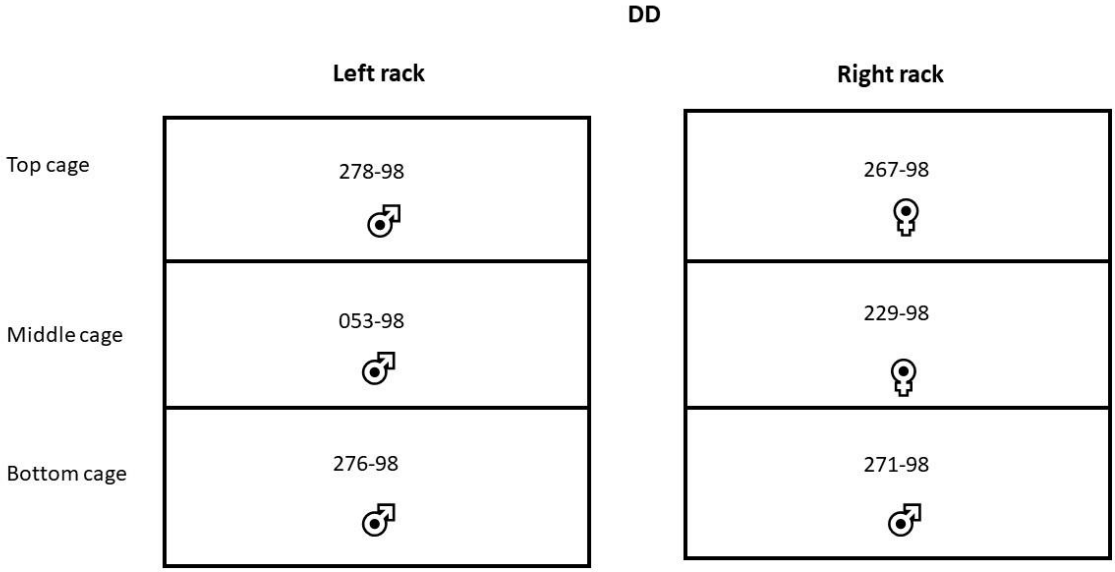

Figure 32 Room plan. The distribution of the experimental group under DD with their identifications and gender.

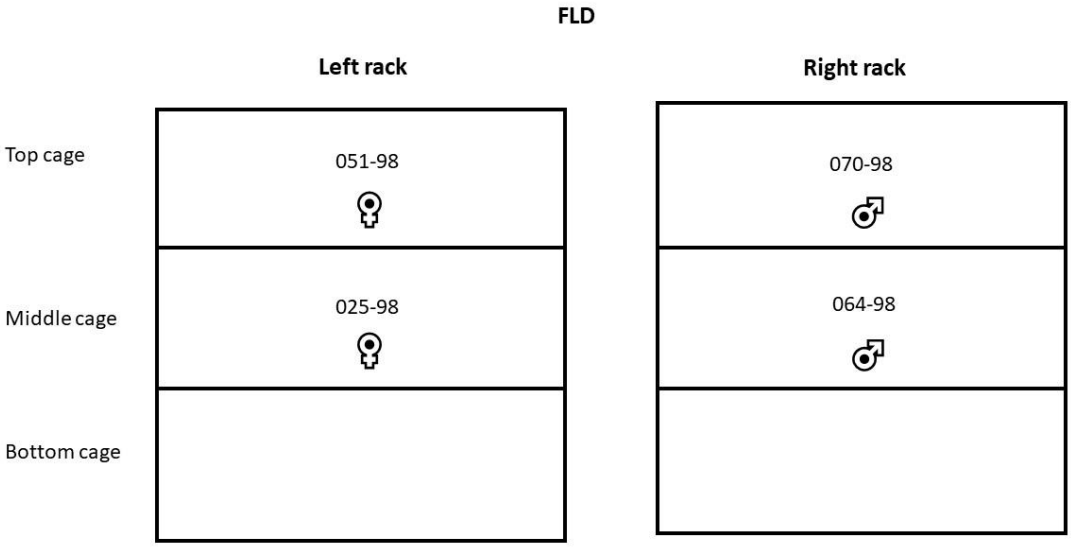

Figure 33 Room plan. The distribution of the birds in the FLD group with their identifications and gender.

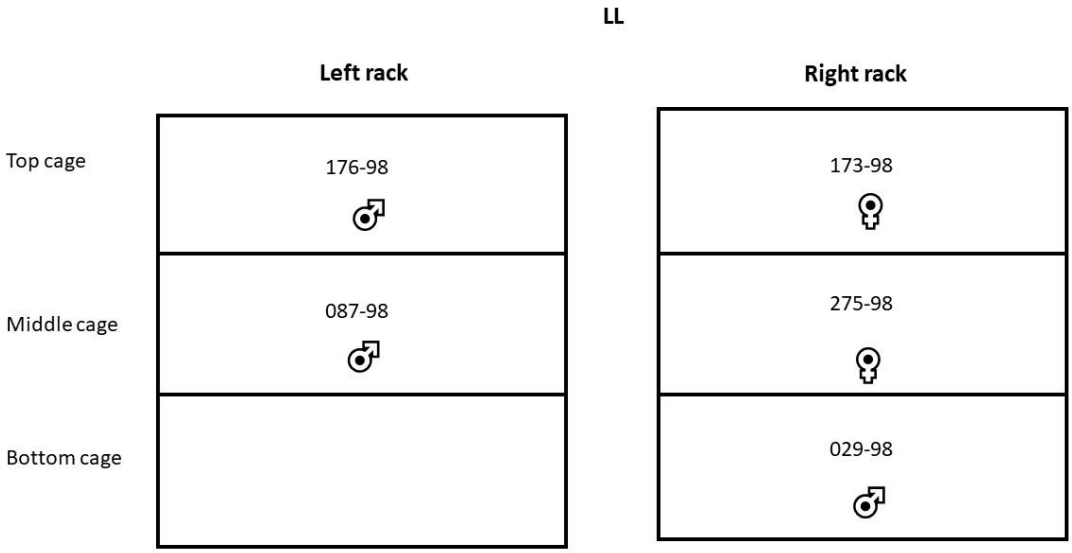

Figure 34 Room plan. The distribution of the experimental group in LL with their identifications and gender.

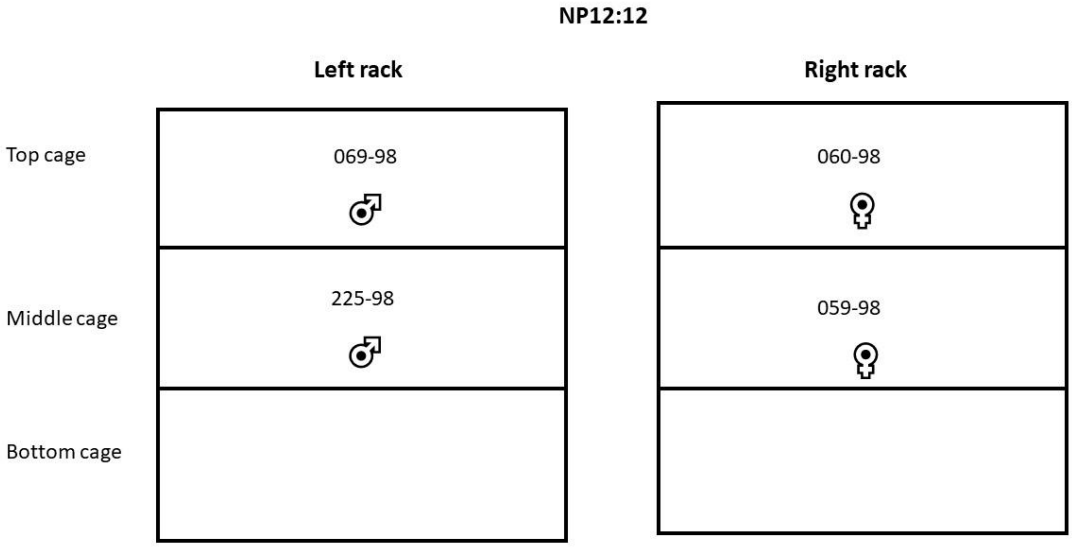

Figure 35 Room plan. The distribution of the experimental group under NP12:12 with their identifications and gender.

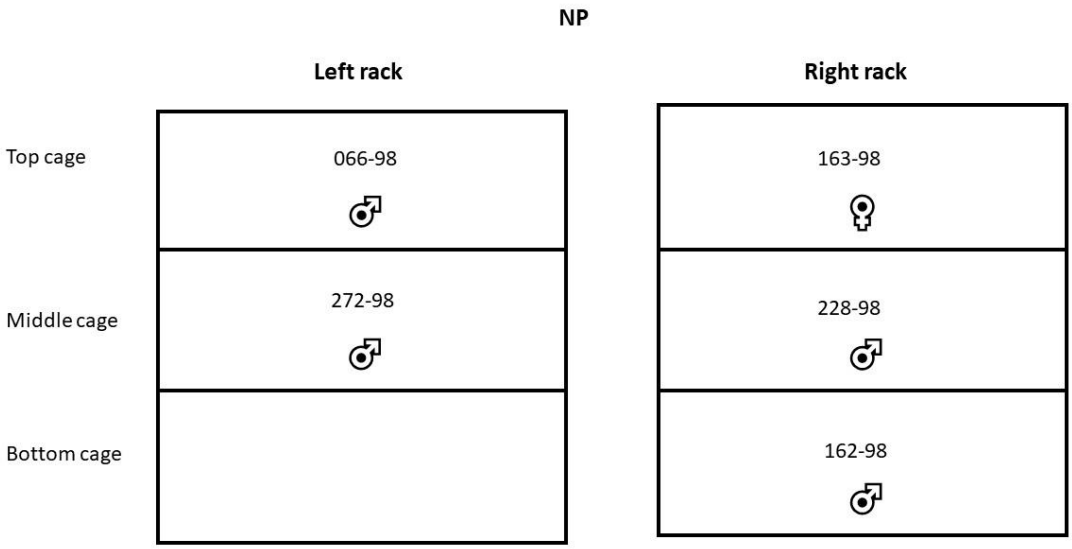

Figure 36 Room plan. The distribution of the experimental group under NP with their identifications and gender.